CHANGES IN REACTIVITY IN A SUBCRITICAL ASSEMBLY OWING TO LOCALIZED PERTURBATIONS

DONALD MILLER BECK

CHANGES IN REACTIVITY IN A SUBCRITICAL ASSEMBLY OWING TO LOCALIZED PERTURBATIONS

by

Donald Miller Beck

A Thesis Submitted to the
Graduate Faculty in Partial Fulfillment of
The Requirements for the Degree of
MASTER OF SCIENCE

Major Subject: Nuclear Engineering

TABLE OF CONTENTS

I. INTRODUCTION

The nuclear properties of a proposed reactor design are often obtained from exponential experiments since nuclear reactor theory is not sufficiently developed to guarantee precise results. Theory is used to calculate lattice constants that are adequate in searching for a lattice with desired nuclear properties, and these calculations will determine the general design and the approximate values of the critical dimensions. Exponential experiments are then carried out to determine more accurately the various lattice constants in order to find more exact values of the critical dimensions.

Reactivity changes owing to localized perturbations, such as the addition of extra fissionable material or poisons, are of considerable interest in many cases of reactor operation, particularly in the safety and control of a reactor. The change in reactivity due to small uniform changes in reactor composition can be estimated by standard group theory or perturbation theory. For small non-uniform or localized changes, standard theory is inapplicable whereas perturbation theory may be used. Perturbation theory has been developed for critical reactors and is used extensively to predict the effect of a proposed addition of fuel or poison to the core of a reactor.

The purpose of this thesis was to investigate the change

in reactivity in a subcritical assembly owing to localized perturbations. The perturbations considered were the addition of fuel, poison and the introduction of a void. The reactivity was obtained experimentally using the formula

$$\rho = \frac{k_e - 1}{k_e} \qquad (1)$$

The theoretical analysis was carried out entirely by perturbation theory. The experimental and theoretical results were correlated to ascertain the feasibility of predicting reactivity changes in a subcritical assembly.

II. REVIEW OF LITERATURE

The development of perturbation theory in reactor calculations is credited by Glasstone and Edlund (1) to E. P. Wigner. The theoretical calculations of reactivity changes by use of perturbation theory were covered in detail by Weinberg and Wigner (2) in which the validity and limitations of perturbation theory were emphasized. The main points presented were that perturbation theory can be trusted without further detailed analysis only if both the effective multiplication factor and the neutron distribution undergo only relatively small fractional changes everywhere. The results of perturbation calculations are always considered to be unreliable if the calculations indicate large changes, whether or not the actual changes are large. It was pointed out that the drawback of almost all perturbation theories is that it is difficult to decide whether the perturbation is small.

A development of perturbation theory was given by McMurry (3) in 1952; however, it was not declassified until December, 1954. He later revised this work and extended the theory to reflected reactors (4). Webster (5) compared the results of two-group perturbation theory and standard two-group theory for uniform changes in composition and concluded that perturbation theory, in almost every case, predicted a greater change than standard two-group theory. In addition, he derived equivalent methods of expressing reactivity

changes used in Fermi age theory, standard group theory, perturbation theory and experimental work. He also investigated weighting factors for calculating reactivity changes (6) and found reasonably good agreement between theoretical and experimental results for a pure absorber. The weighting factor for fuel was determined theoretically, but no experimental verification was presented. The weighting factors for fuel and poisons were computed to be the same at the center of the assembly, while near the sides of the assembly the weighting factor for the absorber was smaller than the weighting factor for the fuel.

Murray (7) developed a method of comparing the reactivity effect of a localized and distributed poison using one-group perturbation theory. Galanin (8) presented a detailed coverage of perturbation theory as used by Soviet scientists.

III. LIST OF SYMBOLS

Symbol	Units	Meaning
a	in, cm	Dimension of assembly plus extrapolation lengths, along x-axis
b	in, cm	Dimension of assembly plus extrapolation lengths, along y-axis
B^2	in^{-2}, cm^{-2}	Buckling
c	in, cm	Dimension of assembly plus extrapolation lengths, along z-axis
C		Constant of proportionality (see equation 17)
D	cm	Diffusion coefficient
e	2.718 . . .	Base of natural logarithms
f		Thermal utilization factor
F		F(x,y,z) (see equation 31)
k		Infinite multiplication factor
k_e		Effective multiplication factor
L	cm	Thermal diffusion length
N	nuclei/cm^3	Nuclei per unit volume
p		Resonance escape probability
R		Ratio of F_1/F_2 (see equation 32)
S	neutrons/sec	Source strength
t	sec	Time
T	sec	Reactor period
U		Uranium

Symbol	Units	Meaning
v	cm/sec	Neutron velocity
V	in^3, cm^3	Volume
x	in, cm	Distance in x direction from origin
y	in, cm	Distance in y direction from origin
z	in, cm	Distance in z direction from origin
γ	in^{-1}, cm^{-1}	Inverse relaxation length
δ		Change in a parameter
Δ		Increment
ε		Fast fission factor
η		Primary fission factor
λ	cm	Mean free path of neutrons
ν	sec^{-1}	Inverse period of reactor
π	3.14159 . . .	Pi
ρ		Reactivity
σ		Standard deviation
Σ	cm^{-1}	Macroscopic cross section
τ	cm^2	Fermi age for neutrons
ϕ	neutrons/sec cm^2	Thermal neutron flux
∇^2		Laplacian operator

Superscripts

Superscript	Meaning
P	Poison
U	Uranium

Superscript	Meaning
'	Changed condition

Subscripts

Subscript	Meaning
a	Absorption
g	Geometric or moderator
i	ith term of a series
m	Material or indicates order of harmonic
n	New value or indicates order of harmonic
o	Origin
p	Perturbed
P	Poison
t	Transport
U	Uranium fuel
V	Volume
1	24 in. level or position 1
2	48 in. level or position 2

IV. THEORETICAL ANALYSIS

A. Perturbation Theory

Perturbation theory involves the series expansion of properties of reactors such as multiplication factors and neutron distributions (2, p. 537). The first term in the series expansion is proportional to the perturbation itself, the second term is proportional to the second power of the perturbation and so on. Due to the difficulty in the calculation of higher order terms, only the first term of the series is generally retained. Therefore, in order to obtain valid results using the first order approximation of the theory, the non-uniform change in the properties of a reactor must be small.

The following analysis is based upon first-order perturbation theory for a critical reactor. It is postulated that in a large subcritical assembly in a region far from the extraneous source where essentially all the neutrons have resulted from fission, the effect of introducing perturbations is the same as in a critical assembly. The one-group model of neutron motion is used and the effect of delayed neutrons is not considered.

B. Poison

The effect of adding a poison was determined using the

method given by Murray (7, p. 231), which is given below. The steady state neutron flux for a critical reactor is given by the equation

$$D\nabla^2\phi + (k-1)\Sigma_a\phi = 0 \qquad (2)$$

When a poison is added or removed the absorption cross section, Σ_a, and the infinite multiplication factor, k, in Equation 2 are changed, resulting in a new value of the coefficient of ϕ equal to $(k'-1)\Sigma_a'$. If the diffusion coefficient remains constant, the time-dependent equation is

$$D\nabla^2\phi' + (k'-1)\Sigma_a'\phi' = \frac{1}{v}\frac{\partial\phi'}{\partial t} \qquad (3)$$

for a bare reactor where v is the velocity of the neutrons. The flux will then increase or decrease with a period T, the reciprocal of which is τ, so that

$$\frac{\partial\phi'}{\partial t} = \frac{\phi'}{T} = \tau\phi' \qquad (4)$$

If

$$(k-1)\frac{\Sigma_a}{D} = B^2 , \qquad (5)$$

then Equation 2 can be rewritten for the changed condition as

$$\nabla^2\phi' = -B'^2\phi' \qquad (6)$$

For an all thermal neutron reactor, the effective multiplication factor, k_e, is

$$k'_e = \frac{k'}{1 + B'^2 L'^2} \tag{7}$$

where

$$L'^2 = \frac{D}{\Sigma'_a} \tag{8}$$

The use of Equations 4, 6, 7 and 8 allows Equation 3 to be written

$$k' \Sigma_a v \frac{\delta k'_e}{k'_e} \phi' = \nu \phi \ , \tag{9}$$

where $\delta k'_e = k'-1$ and thus $\delta k'_e/k'_e$ is equal to the reactivity from Equation 1 for the changed condition. If Equation 9 is multiplied by the original flux distribution ϕ and integrated over the reactor volume, V, the result is

$$\frac{\delta k'_e}{k'_e} \int_V k' \Sigma'_a v \phi\phi' dV = \nu \int_V \phi\phi' dV \tag{10}$$

The neutron velocity v and inverse period ν can be eliminated and $\delta k'_e/k'_e$ solved for by the following procedure. Multiplying Equation 2 by ϕ' gives

$$\phi' D \nabla^2 \phi + (k-1) \Sigma_a \phi\phi' = 0 \tag{11}$$

Multiplying Equation 3 by ϕ and using the relationship given in Equation 4 gives

$$\phi D \nabla^2 \phi' + (k'-1) \Sigma'_a \phi\phi' = \frac{\nu}{v} \phi\phi' \tag{12}$$

If Equation 11 and 12 are subtracted and then integrated over

the volume of the assembly, V, the terms containing ∇^2 vanish since their solution leads to a complete set of eigenfunctions that are orthogonal over the reactor volume (1, p. 373). The resulting equation is

$$\int_V v \quad \delta\left[(k-1)\,\Sigma_a\right] \quad \phi\phi'dV = \nu\int_V \phi\phi'dV \quad (13)$$

where $\delta\left[(k-1)\,\Sigma_a\right]$ is the change in this parameter. Equating the left side of Equations 10 and 13 gives the desired result

$$\rho = \frac{\delta k'_e}{k'_e} = \frac{\int_V \delta\left[(k-1)\,\Sigma_a\right]\,\phi\phi'dV}{\int_V k'\,\Sigma'_a\phi\phi'dV} \quad (14)$$

The special case is considered by Murray (7, p. 232) in which a poison is added, but the cross section of the fuel, Σ_a^U, is unchanged. Now $k = \eta\varepsilon pf$ (cf. Section VI.D.1). For the addition of a poison, only f is changed (c.f. Section VI.D.3); therefore, since $f = \Sigma_a^U/\Sigma_a$ the quantity $k\,\Sigma_a = \eta\varepsilon p\,\Sigma_a^U$ is a constant. For this case, $\delta\left[(k-1)\,\Sigma_a\right] = -\,\delta\Sigma_a$ in Equation 14. If the disturbed flux ϕ' and the original flux ϕ are assumed to be approximately the same, Equation 14 can be written

$$\rho = \frac{\delta k'_e}{k'_e} = \frac{-\int_V \left(\delta\Sigma_a\right)\phi^2 dV}{\int_V k\,\Sigma_a\phi^2 dV} \quad (15)$$

which gives the absorption reactivity by perturbation theory.

The absorption reactivity is thus seen to be proportional to a "weighting" factor of ϕ^2.

The change in reactivity due to localized poisons was found theoretically by a comparison of localized and distributed poisons and the ratio of reactivity of the same poison in two positions. The following development is based upon the method presented by Murray (7, p. 232).

The reactivity due to a localized poison of volume V_p and cross section Σ_a^P located at a position (x,y,z) is proportional to $V_p\Sigma_a^P\phi^2$ if the volume of the poison, V_p, is small enough that $\int_{V_p} \phi^2 dV = V_p\phi^2$, where ϕ is the neutron flux at the position of the poison. For an exponential assembly with dimensions a, b and c, including the extrapolation distances

$$\phi^2 = \phi_o^2 \cos^2 \frac{\pi x}{a} \cos^2 \frac{\pi y}{b} e^{-2\gamma z} \qquad (16)$$

where ϕ_o is the flux at the origin. The reactivity for a localized poison in an exponential assembly is

$$\rho = CV_p\Sigma_a^P\phi_o^2 \cos^2 \frac{\pi x}{a} \cos^2 \frac{\pi y}{a} e^{-2\gamma z} \qquad (17)$$

where C is a constant of proportionality.

The ratio of the reactivities, R.C.R., for the same poison in two positions (x_1, y_1, z_1) and (x_2, y_2, z_2), can be found from the ratio of Equation 17 for the two positions, which gives

$$R.O.R. = \frac{\cos^2\frac{\pi x_1}{a}\cos^2\frac{\pi y_1}{b}e^{-2\gamma z_1}}{\cos^2\frac{\pi x_2}{a}\cos^2\frac{\pi y_2}{b}e^{-2\gamma z_2}} \qquad (18)$$

where γ is equal to γ for the unperturbed condition since it is assumed in perturbation theory that the change in flux is small.

For a poison uniformly distributed throughout a volume, V, the poison absorption per unit volume is $V_P \Sigma_a^P/V$. The reactivity, found by integration over the volume for an exponential assembly is

$$\rho = C\int_0^c\int_{-b/2}^{b/2}\int_{-a/2}^{a/2}\frac{V_P\Sigma_a^P}{V}\phi_o^2\cos^2\frac{\pi x}{a}\cos^2\frac{\pi y}{b}e^{-2\gamma z}dxdydz \qquad (19)$$

where C is a constant of proportionality.

Integrating Equation 19 with V_P, Σ_a^P and V constant gives

$$\left[\frac{C\phi_o^2 V_P \Sigma_a^P}{8c\gamma}\right](1 - e^{-2\gamma c})$$

The ratio of reactivities for a localized to distributed poison can be obtained by dividing Equation 17 by the above quantity. The result is

$$\left[\frac{8c\gamma}{(1-e^{-2\gamma c})}\right]\cos^2\frac{\pi x}{a}\cos^2\frac{\pi y}{b}e^{-2\gamma z} \qquad (20)$$

C. Fuel

For a relatively large subcritical assembly the thermal neutron flux distribution, at a distance from boundaries and from the extraneous source, can be represented by the one-group equation (1, p. 281)

$$\nabla^2\phi + B^2\phi = 0 \tag{21}$$

where B^2, the material buckling, and ϕ are for the unperturbed condition. If the neutron absorption, or multiplication, is changed in a region of the assembly of volume V_p, the buckling in the perturbed region p is changed to a new value B_p^2. For the changed condition, equation 21 can be written

$$\nabla^2\phi' + B_n^2\phi' = 0 \tag{22}$$

where B_n^2 is the new value of buckling for the entire assembly after the perturbation is introduced.

Using Equations 21 and 22 with a development analogous to that used to obtain Equation 14, Galanin (8, p. 117) gives the change in buckling as

$$B^2 - B_n^2 = (B^2 - B_p^2)\frac{\int_{V_p}\phi^2 dV}{\int_V \phi^2 dV} \tag{23}$$

assuming $\phi' = \phi$. This result, which can be used to determine the buckling due to the addition of fuel, was obtained by

Glasstone and Edlund (1, p. 378) based upon the statistical weight of a region of a large bare reactor.

V. DESCRIPTION OF EQUIPMENT

The Iowa State College subcritical assembly, shown in Figure 1, was used for the experimental investigations. It consisted of 14 layers of graphite blocks, each layer containing ten blocks. The blocks in the lower nine layers were approximately 62 inches long, and had a cross section of 6 in. by 6 in. The blocks in the upper five layers were 60.5 in. long and 6 in. by 5 in. in cross section and were placed with the 6 in. side horizontal. The physical dimensions of the assembly were 79 in. high, 60 in. wide, and 62 in. and 60.5 in. long in the lower nine layers and upper layers respectively. The lower and upper graphite blocks had 3.5 in. and 3.187 in. radii respectively on the corners which provided channels through the assembly in which fuel or measuring equipment could be inserted.

The graphite assembly was covered on the top and sides with 10-mil sheets of cadmium sandwiched between plywood and masonite to provide a "black boundary" to the thermal neutrons. From measured lengths, the dimensions in a horizontal section between cadmium sheets were 61 in. and 63 in. in the x and y directions respectively.

The assembly was mounted on a base which provided a space underneath for insertion of three open topped aluminum water tanks about a foot high. Two tanks extending the length of the assembly were placed on each side of the source. The

Figure 1. Iowa State College subcritical assembly

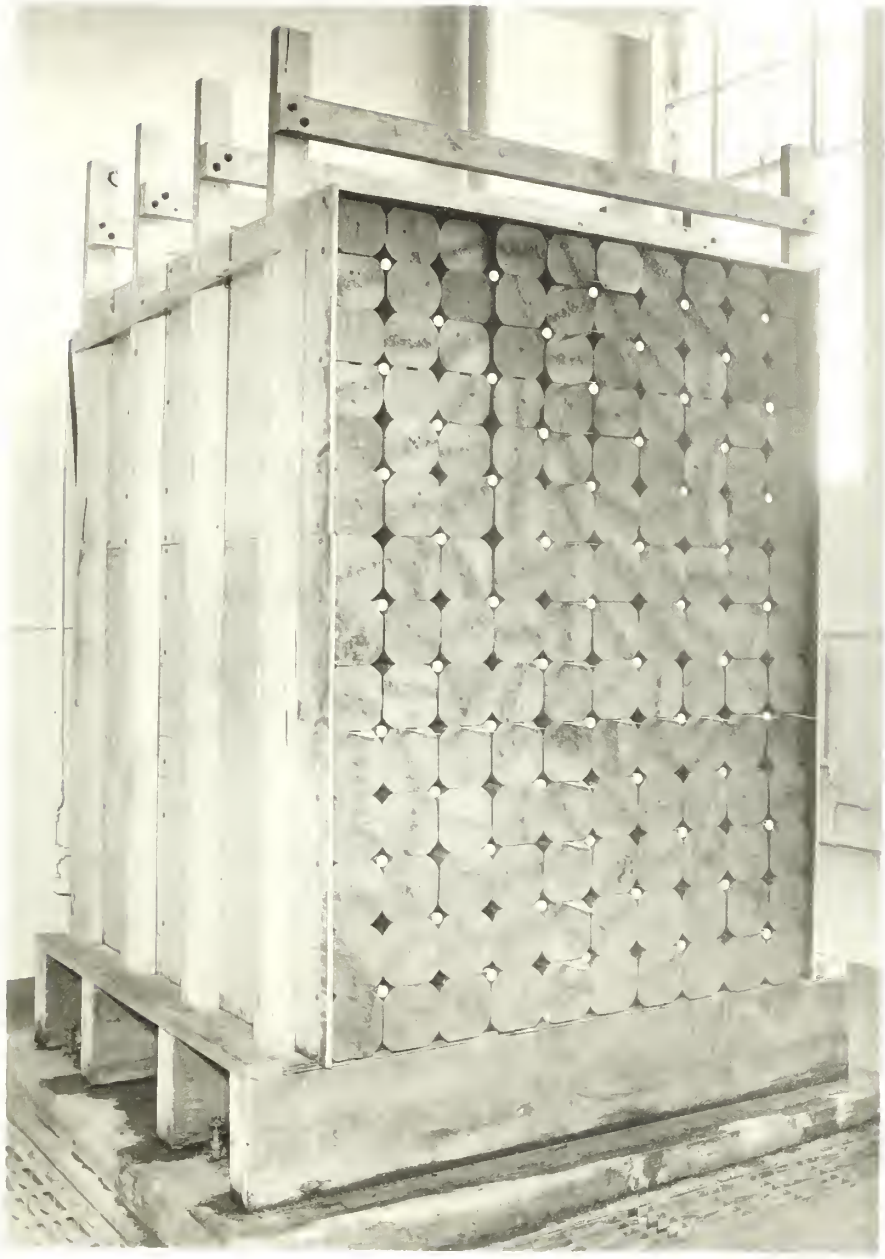

center tank consisted of three compartments. The middle compartment contained a wooden frame on which the sources were mounted.

Five separate plutonium-beryllium neutron sources encased in tantalum and stainless steel cylinders 1.0 in. in diameter and 1.3 in. high, each emitting about 1.63×10^6 neutrons per second, comprised the assembly source. The sources were placed in a cruciform arrangement with the tops of the source cases directly beneath the center of the floor of the assembly.

The fuel was natural uranium in the form of cylindrical rods 1.00 in. in diameter and 8.00 in. long. The rods were encased in 2S aluminum 0.035 in. thick on the sides and 0.200 in. thick on the ends. Thus the overall dimensions of the fuel slugs, which are shown in Figure 2, were 1.080 in. in diameter by 8.40 in. long. Seven fuel slugs were placed in a process tube to form a fuel assembly. The 61S aluminum process tubes were 62 in. long, had an outside diameter of 1.375 in. and a wall thickness of 0.035 in. A 2S aluminum spacing wire, 0.102 in. in diameter and approximately ten feet long, was wrapped around the fuel slugs in each process tube.

A 25.2 in. long by 15/16 in. diameter wood dowel was wrapped with a single thickness of 10-mil cadmium to form a thermal neutron absorber. The ends of the dowel were also

Figure 2. Scaler, counter, absorber and three fuel slugs


RADIATION INSTRUMENT
DEVELOPMENT LABORATORY

covered with cadmium. The overall dimensions of the absorber were approximately the same as three fuel slugs placed end to end as shown in Figure 2.

A BF_3 counter, No. G10917, manufactured by N. Wood Counter Laboratory and a Radiation Instrument Development Laboratory scaler, model 206, were used to measure the thermal neutron flux in the assembly.

The counter probe was 1/2 in. in diameter and ten in. long. The center of the 8 in. active volume was 5 in. from the end of the tube. The overall length of the counter was 15.0 in. and the maximum diameter was 1.0 in. The counter cord was taped and marked at 10, 13, 19, 25 and 31 in. intervals from the center of the active volume to facilitate positioning of the counter in the assembly. The counting equipment is shown in Figure 2.

VI. EXPERIMENTAL INVESTIGATION

A. General Procedure

The experimentation was conducted for a reference configuration and five separate configurations. Horizontal traverses were made at the 24 in. and 48 in. levels for all configurations (Figure 3). The counter was placed in the air holes of the assembly in rows A, B, C, D, and E at the following positions in the y direction: y = 0, $\pm$ 6, $\pm$ 12, $\pm$ 18 and $\pm$ 21 in. (Figure 4). Due to difficulty in accurately positioning the counter near the edge of the assembly, measurements in y = $\pm$ 21 in. positions were discontinued after the first set of runs. Thus counts were taken at 45 positions on each level for the reference configuration and at 35 positions for all subsequent configurations. The counter was placed in the assembly from the face nearest the position measured. The center position in each row was consequently measured twice during each run, once from each direction.

The source compartment was dry while the rest of the tanks were filled with water and the faces of the assembly were in place for all runs. The counting time at each position was three minutes for both levels for the reference configuration. For the other configurations, the counting time was two minutes for the 48 in. level and one minute for

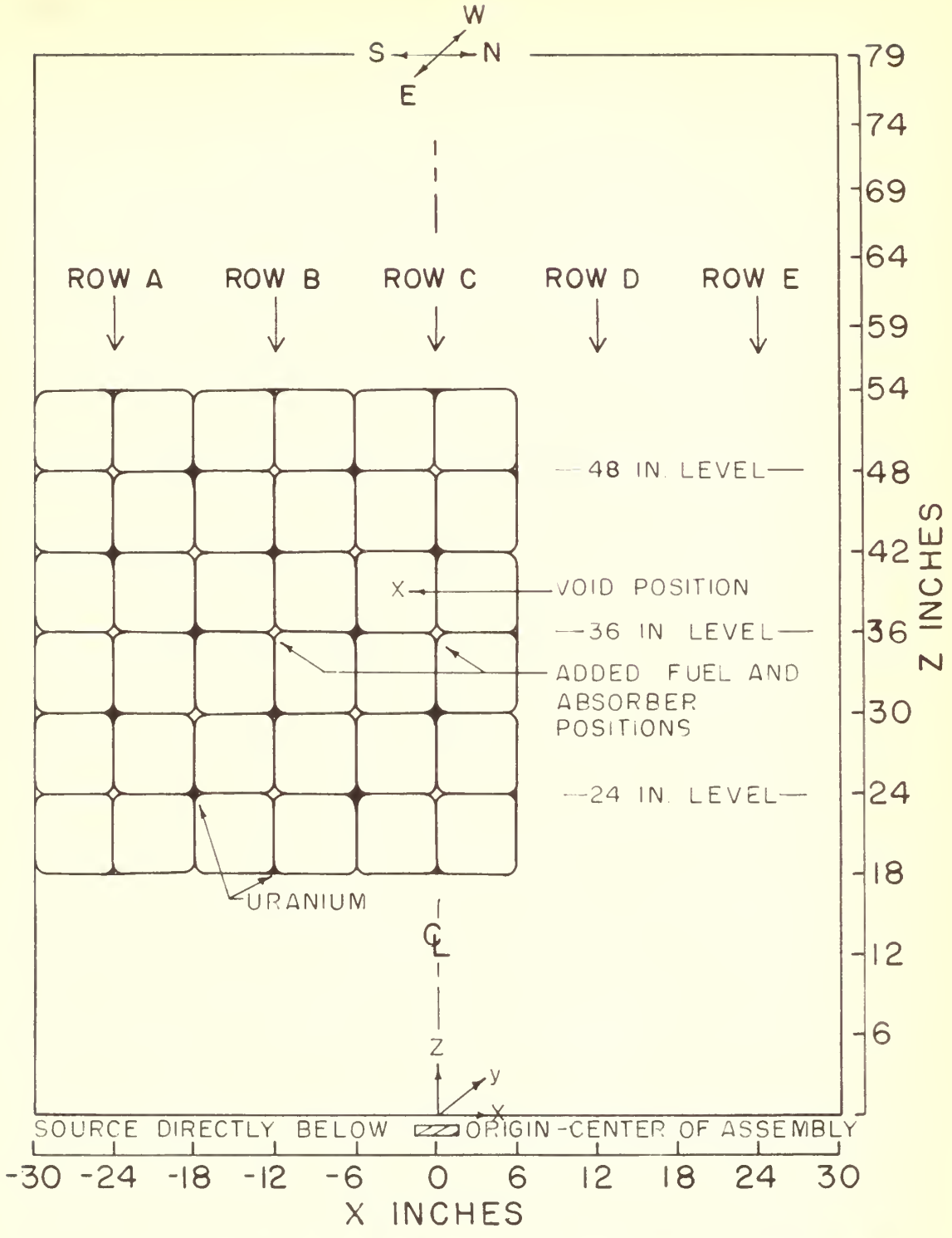

Figure 3. Front view of assembly showing positions of added fuel, poison and void

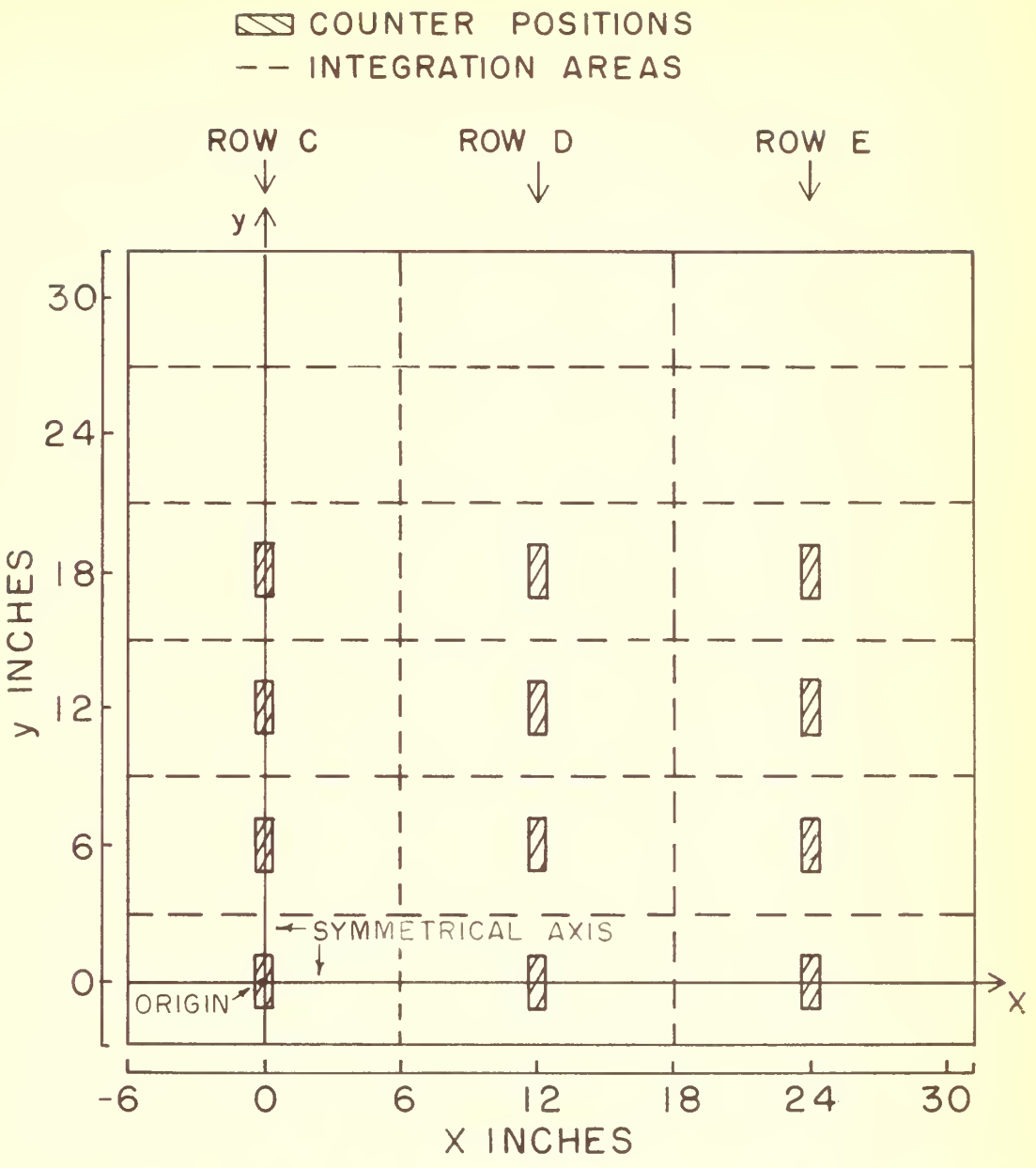

Figure 4. Top view of positive x and y quadrant of assembly showing counter positions and integration areas

the 24 in. level. Deadtime corrections were negligible for all counts.

The center of the active volume of the counter was determined by placing the counter in the center of a row alternately from each face and comparing the counts. The center of the active volume was determined to be 5 in. from the end of the counter and proved to be the same location specified by the manufacturer*. The scaler was operated in the proportional region at 1900 volts with a gain setting of 1.0 and a discriminator setting of 0.50 for all counts.

B. Configurations

For the reference configuration every other hole in the assembly was filled with a fuel assembly, as shown in Figure 1, so that an 8.48 in. square uranium-graphite lattice was formed in the lower region of the assembly.

The first configuration was identical to the reference configuration except that the cadmium absorber (Figure 2) was placed symmetrically about the center of row C in the 36 in. level. Upon completion of the runs for the first configuration, the absorber was removed from row C and placed at the same level in the center of row B for the second configuration.

---

*Wood, N, Chicago, Ill. Active volume of counter. Private communication. 1958.

For configurations 3 and 4 three fuel slugs were placed in the same positions occupied by the absorber for configuration 1 and 2, respectively, as shown in Figure 3.

Configuration 5 was a modification of the reference configuration by removing the entire graphite block at position x = -3 in., z = 39 in. (Figure 3) and replacing it by four 7.25 in. long graphite blocks. The small blocks were placed together in pairs at each end of the row so that a 6 in. by 6 in. by 31 in. void was thus introduced in the center of the assembly. The small graphite blocks had a cross section of 5 in. by 6 in. and were placed with the 5 in. side horizontal. This resulted in small air gaps along each side of the blocks.

C. Inverse Relaxation Length

The immediate object of the measurements for each configuration was to evaluate γ, the inverse relaxation length of the neutron flux in the z direction. A method suggested by R. E. Uhrig* was used to find γ. The details of the method are as follows.

In a subcritical assembly with a single extraneous source

---

*Uhrig, R. E., Iowa State College, Ames, Iowa. Method of measuring material buckling in a subcritical assembly. Private communication. 1958.

of strength S in the center of the pedestal, the steady state flux, ϕ, at any point (x,y,z), not too near the extraneous source or boundaries, is

$$\phi(x,y,z) = \frac{2S}{abD} \sum_{m=1}^{\infty} \sum_{n=1}^{\infty} \frac{1}{\gamma_{mn}} \cos\frac{m\pi x}{a} \cos\frac{n\pi y}{b} e^{-\gamma_{mn} z} \left[1-e^{-2\gamma_{mn}(c-z)}\right] \tag{24}$$

where D is a diffusion constant, c is the vertical dimension (including the extrapolated distance) of the assembly, and m and n are odd integers indicating the order of harmonic. If each side of Equation 24 is multiplied by $\cos\frac{\pi x}{a} \cos\frac{\pi y}{b} dxdy$ and the quantities involving x and y are integrated over the limits -a/2 to a/2 and -b/2 to b/2 respectively, the resulting equation is

$$\int_{-a/2}^{a/2} \int_{-b/2}^{b/2} \phi(x,y,z) \cos\frac{\pi x}{a} \cos\frac{\pi y}{b} dxdy = \int_{-a/2}^{a/2} \int_{-b/2}^{b/2} \frac{2S}{abD} \sum_{m=1}^{\infty} \sum_{n=1}^{\infty} \frac{1}{\gamma_{mn}} \cos\frac{m\pi x}{a} \cos\frac{\pi x}{a} \cos\frac{n\pi y}{b} \cos\frac{\pi y}{b} e^{-\gamma_{mn} z}\left[1-e^{-2\gamma_{mn}(c-z)}\right] dxdy \tag{25}$$

The functions on the right side of Equation 25 form an orthogonal set over the intervals -a/2 to a/2 and -b/2 to b/2 and thus all terms having $m \neq 1$ and $n \neq 1$ will be zero. Consequently all the harmonic terms are eliminated and the

double infinite summation is reduced to a single term. After integration of the right side, Equation 25 becomes

$$\int_{-a/2}^{a/2}\int_{-b/2}^{b/2} \phi(x,y,z)\cos\frac{\pi x}{a}\cos\frac{\pi y}{b}dxdy = \frac{S}{2\gamma D}\, e^{-\gamma z}\left[1-e^{-2\gamma(c-z)}\right] \tag{26}$$

Since γ_{mn} is equal now to γ_{11}, the subscript is dropped. By definition,

$$F(x,y,z) = \int_{-a/2}^{a/2}\int_{-b/2}^{b/2} \phi(x,y,z)\cos\frac{\pi x}{a}\cos\frac{\pi y}{b}dxdy \tag{27}$$

then for level z_1

$$F(x,y,z_1) = \frac{S}{2\gamma D}\, e^{-\gamma z_1}\left[1 - e^{-2\gamma(c-z_1)}\right] \tag{28}$$

and for level z_2

$$F(x,y,z_2) = \frac{S}{2\gamma D}\, e^{-\gamma z_2}\left[1 - e^{-2\gamma(c-z_2)}\right] \tag{29}$$

Division of Equation 28 by Equation 29 gives

$$\frac{F(x,y,z_1)}{F(x,y,z_2)} = e^{-\gamma(z_1-z_2)}\left\{\frac{1-e^{-2\gamma(c-z_1)}}{1-e^{-2\gamma(c-z_2)}}\right\} \tag{30}$$

Hereafter,

$$F(x,y,z) = F \tag{31}$$

and

$$\frac{F_1}{F_2} = R \tag{32}$$

The terms F_1 and F_2 for levels z_1 and z_2 can be obtained using graphical or tabular methods of integration after neutron measurements have been taken at grid points on the two levels. The terms in the brackets of Equation 30 are the end correction factors and are nearly equal to unity if the levels z_1 and z_2 are not too near the top of the assembly. Hence, Equation 30 can be simplified to give a first approximation of γ as

$$= \frac{\ln \left[\frac{F_1}{F_2}\right]}{(z_2 - z_1)} \tag{33}$$

The F terms for the 24 in. and 48 in. levels, hereafter referred to as F_1 and F_2 respectively, were evaluated using the approximation

$$\int_{-a/2}^{a/2} \int_{-b/2}^{b/2} \phi(x,y,z) \cos \frac{\pi x}{a} \cos \frac{\pi y}{b} \, dxdy = \sum_{-a/2}^{a/2} \sum_{-b/2}^{b/2} \phi(x,y,z) \cos \frac{\pi x}{a} \cos \frac{\pi y}{b} \, \Delta x \, \Delta y \tag{34}$$

The grid system used to evaluate the F terms is shown in Figure 4. The dimensions a and b, which include the extrapolated distances, were found from Figures 5 through 8 by measuring the distance between the positions for the flux equal to zero, as described in reference 1, p. 285. The

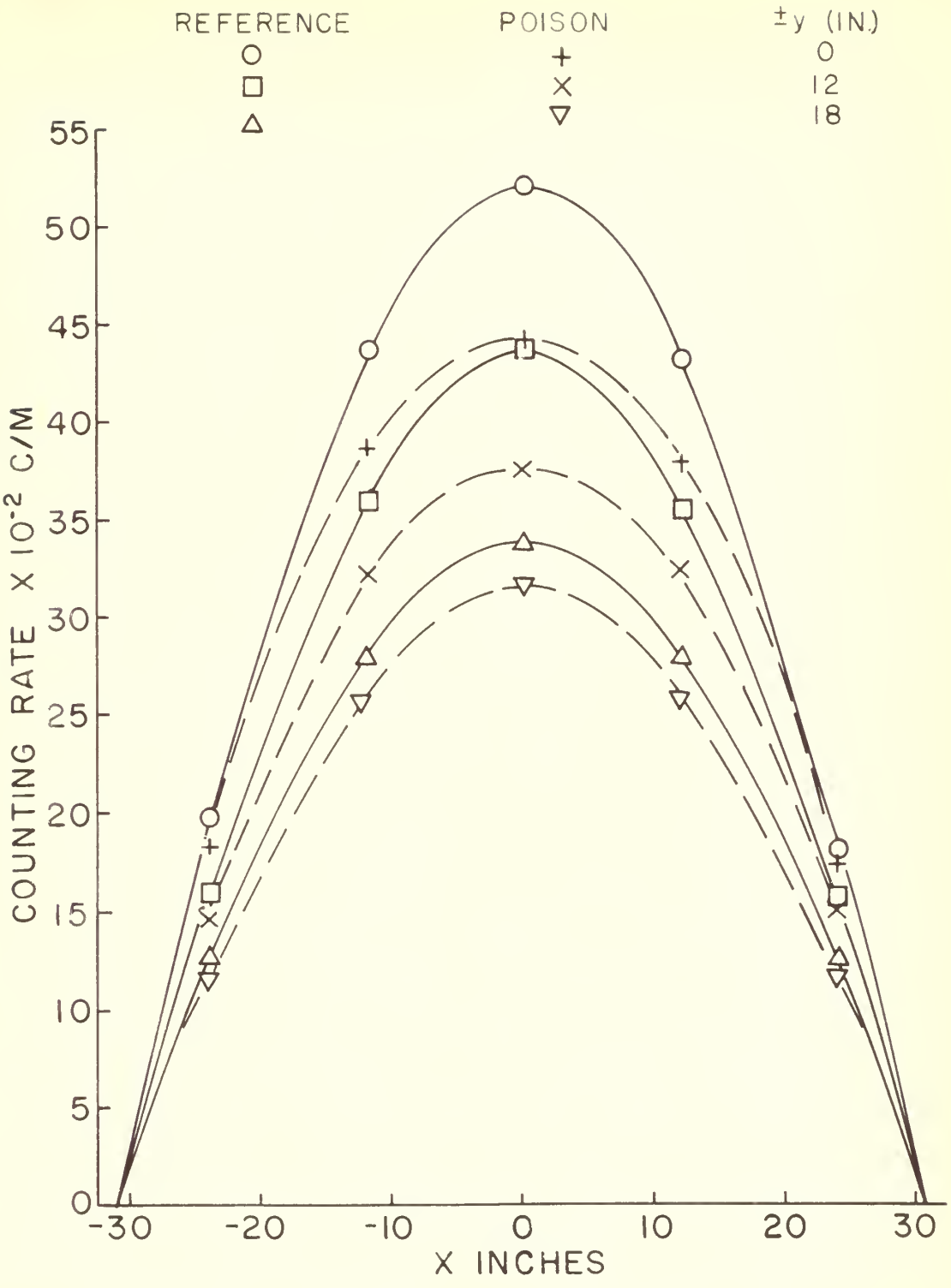

Figure 5. Horizontal flux survey, 48 in. level, configuration 1

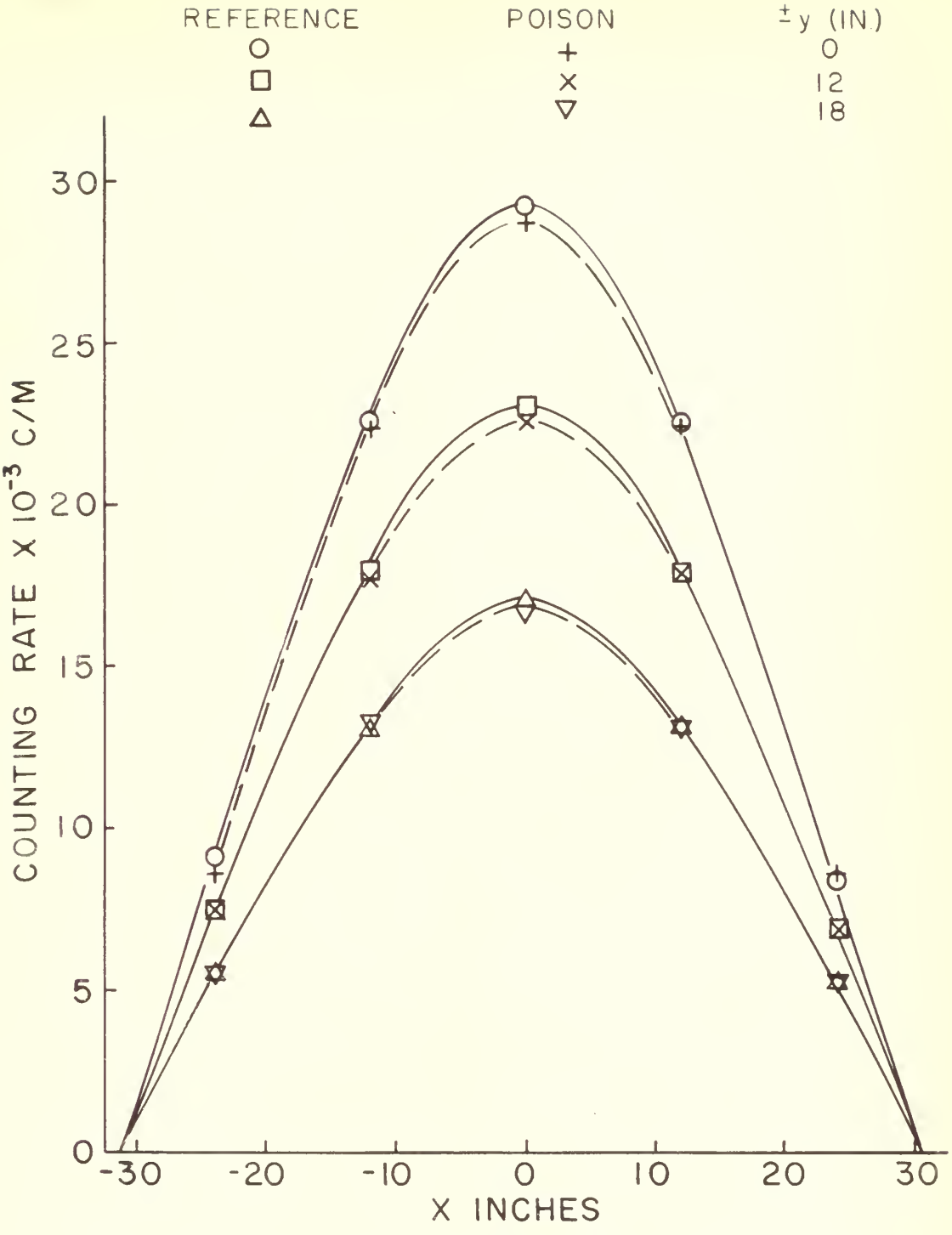

Figure 6. Horizontal flux survey, 24 in. level, configuration 1

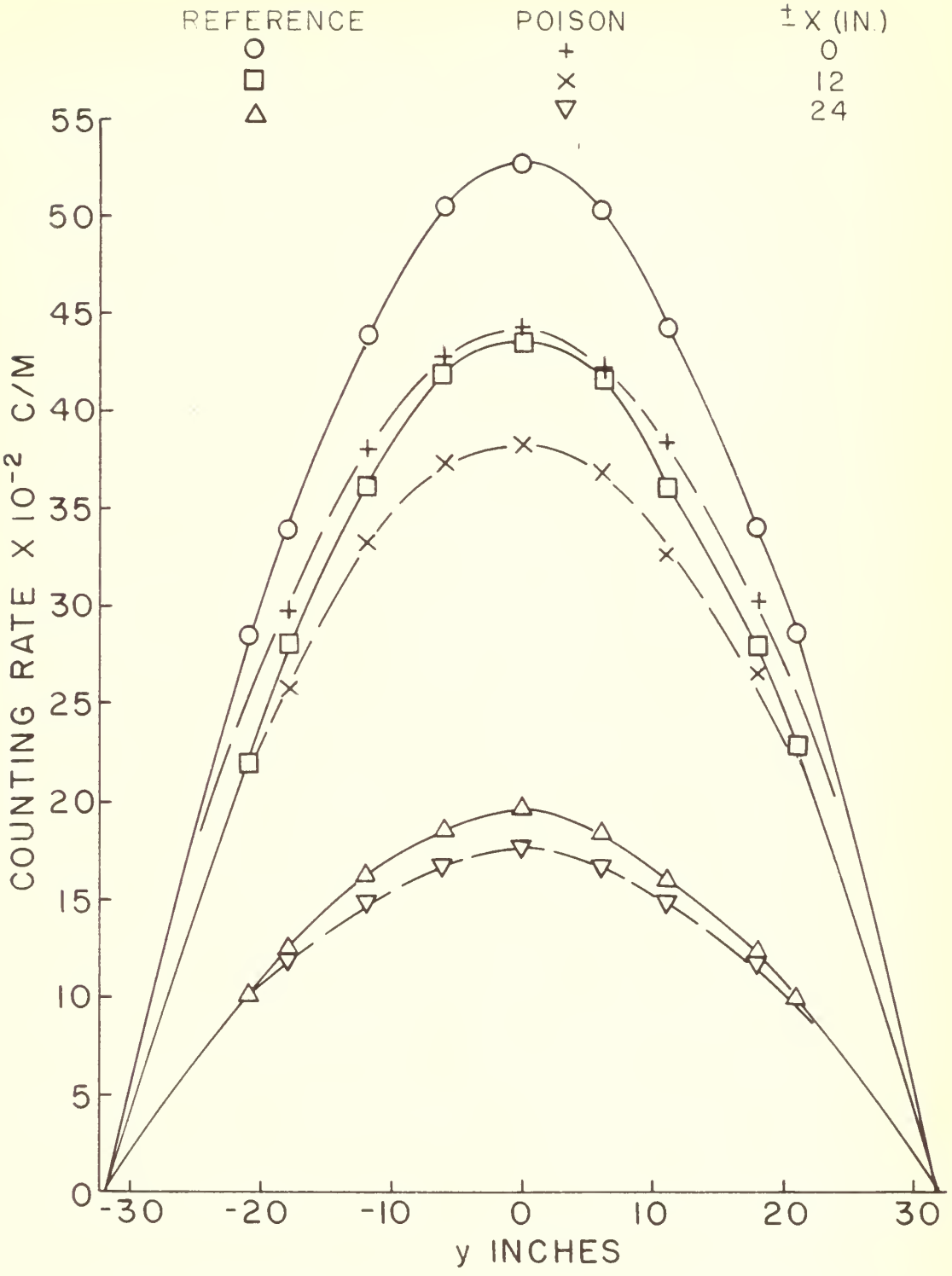

Figure 7. Horizontal flux survey, 48 in. level, configuration 1

Figure 8. Horizontal flux survey, 24 in. level, configuration 1

dimensions a and b were found to be 62 and 54 in. respectively. The positions of the neutron flux measurements correspond to the center of the $\Delta x \Delta y$ areas as shown by dashed lines in Figure 4. The values of the neutron flux at the center of the $\Delta x \Delta y$ areas for $y = \pm 24$ in. and $y = \pm 29.5$ in. in Table 1 were obtained by multiplying the value of the neutron flux at $y = \pm 18$ in. by a factor of 0.60 and 0.20, respectively. These factors were determined from the plot of neutron flux versus y in Figures 7 and 8.

The summation process used to obtain F_1 and F_2 for each configuration was carried out by tabulation and summation of $\phi(x,y,z) \cos \frac{\pi x}{a} \cos \frac{\pi y}{b} \Delta x \Delta y$ terms. The values $\cos \frac{\pi x}{a} \cos \frac{\pi y}{b} \Delta x \Delta y$ are listed in Table 1. The values of the measured counting rates, which are proportional to the neutron flux $\phi(x,y,z)$, are given in Appendix B for the reference configuration. The resultant values for F_1 and F_2 and R are

Table 1. Values of $\cos \frac{\pi x}{a} \cos \frac{\pi y}{b} \Delta x \Delta y$

$\pm$ y (in.)	Row A	Row B	Row C	Row D	Row E
0.0	0.163	0.410	0.500	0.410	0.163
6.0	0.156	0.392	0.478	0.392	0.156
12.0	0.135	0.341	0.416	0.341	0.135
18.0	0.103	0.259	0.317	0.259	0.103
24.0	0.062	0.156	0.191	0.156	0.062
29.5	0.0163	0.0412	0.0501	0.0412	0.0163

given in Table 2.

These values of F_1 and F_2 were substituted into Equation 33, and an approximate value of γ was obtained. An iteration process was then performed using Equation 30 to obtain the final values of γ given in Table 2 for each configuration.

Table 2. Inverse relaxation length

Configuration	F_1	F_2	R	γ(in.$^{-1}$)
Reference	185,358	36,442	5.01	0.0671
1	182,369	32,296	5.65	0.0718
2	186,550	33,770	5.54	0.0708
3	187,417	36,272	5.17	0.0680
4	186,795	36,524	5.11	0.0675
5	185,655	39,069	4.75	0.0644

To ascertain the precision of the calculated values of γ, the standard deviation of the inverse relaxation lengths were computed as shown in Appendix A.

With the inverse relaxation length known, the material buckling, B_m^2, for a rectangular, exponential assembly can be obtained from (1, p. 283)

$$B_m^2 = \left(\frac{\pi}{a}\right)^2 + \left(\frac{\pi}{b}\right)^2 - \gamma^2 \qquad (35)$$

With the values of a and b of 62 and 64 in. respectively,

(found above), Equation 35 becomes

$$B_m^2 = 772 \times 10^{-6} - \gamma^2 \qquad (36)$$

where the units of B_m^2 are cm^{-2}.

The values of the material buckling were computed for each configuration using Equation 36 and values of γ listed in Table 2. The value of B_m^2 for each configuration is given in Table 3.

D. Reactivity Changes

1. General

The definition of reactivity as given by Equation 1 is

$$\rho = \frac{k_e - 1}{k_e} \qquad (1)$$

For the experimental investigation the determination of reactivity consisted in the determination of the effective multiplication factor, k_e, by use of modified one-group theory.

The effective multiplication factor of a reactor is the average number of thermal neutrons remaining in a reactor after one generation for each initial neutron absorbed. For a bare, homogeneous, thermal reactor, the effective multiplication factor may be defined by (1, p. 199)

$$k_e = \frac{k\, e^{-B_g^2 \tau}}{1 + L^2 B_g^2} \qquad (37)$$

where τ is the Fermi age for the thermal neutrons. The Fermi age was assumed to be equal to that in the pure moderator (1, p. 280). Murray (7, p. 123) gives the value of τ of 364 cm^2 for graphite. The geometric buckling, B_g^2, is related to the shape and dimensions, a, b, and c of an assembly. For a rectangular parallelepiped assembly, the geometric buckling is

$$B_g^2 = \left(\frac{\pi}{a}\right)^2 + \left(\frac{\pi}{b}\right)^2 + \left(\frac{\pi}{c}\right)^2 \qquad (38)$$

where a, b, and c include the extrapolation distances. The vertical dimension, c, of 79.75 in. was found by adding an extrapolation length of 0.71 λ_t to the measured height of the assembly (Table 4). This value for c and values of a and b of 62 in. and 64 in. respectively (Table 4) were substituted into Equation 38 and the value of B_g^2 was found to be 1014 x 10^{-6} cm^{-2}.

The infinite multiplication factor, k, is equal to the product of the primary fission neutron factor, η, the fast fission factor, ε, the resonance escape factor, p, and the thermal utilization factor, f. That is,

$$k = \eta \varepsilon p f \qquad (39)$$

For a large reactor, k can be found from the critical equa-

tion (1, p. 216)

$$k = 1 + B_m^2 (L^2 + \tau) \qquad (40)$$

where $B_g^2 = B_m^2$ for the critical condition. The thermal diffusion length in the assembly, L^2, is

$$L^2 = L_g^2 (1 - f) \qquad (41)$$

where L_g^2 is the thermal diffusion length in pure moderator. Murray (7) gives a value of L_g^2 of 2,520 cm^2. Both k and L^2 were evaluated for each configuration by use of Equations 39 through 41, as shown in the following subdivisions.

With the evaluated quantities k and L^2 and the known constant values of B_g^2 and τ, k_e was found from Equation 37 and substituted into Equation 1 to obtain the reactivity for each configuration.

2. Reference configuration

For the 8.48 in. lattice used in the reference configuration, the value of L^2 given by Hoganson (9, p. 56) is 345 cm^2. This value was used in Equation 40, with the value of B_m^2 from Table 3, to obtain k. The effective multiplication factor and the reactivity were then found from Equations 37 and 1 respectively. The values are given in Table 3.

3. Poison

The only factors in the above equations that change sig-

nificantly due to the addition of an absorber, or poison, are B_m^2, f and L^2 (7, p. 105). The factors η, ϵ, and p in Equation 39 are considered to be constant. The product of $\eta \epsilon p$ was calculated using Equation 39 with the known values of k and f for the reference configuration, that is

$$\eta \epsilon p = \frac{k}{f} = \text{constant} \qquad (42)$$

The thermal utilization factor for the added poison was then obtained using Equations 40 through 42 with values of B_m^2 for configurations 1 and 2 given in Table 3. The value of k was calculated from Equations 40 and 41 and then the values of k_e and ρ were found from Equations 37 and 1 respectively. These values for configurations 1 and 2 are given in Table 3.

If the neutron flux in the poison and fuel are considered to be the same, the thermal utilization factor for a uniformly distributed poison, f', can be obtained from

$$\frac{1}{f'} = \frac{1}{f} + \frac{V_P N_P \sigma_a^P}{V_U N_U \sigma_a^U} \qquad (43)$$

where N_P, N_U and σ_a^P, σ_a^U are the number of nuclei per unit volume of the pure material and the microscopic cross section respectively, of the poison, P, and the fuel, U. The thermal utilization f is for the unperturbed condition. The reactivity can be determined using the same procedure outlined above. The values used in Equation 43 are given in Table 4. The values of f' and ρ were calculated to be 0.782 and -1.34

respectively.

4. Fuel

The change in the thermal diffusion length was assumed to be negligible due to the addition of fuel, configurations 3 and 4. The value of k was calculated using Equation 40 with the value of B_m^2 for configurations 3 and 4 from Table 3 and the value of L^2 for the reference configuration (Table 4). The values of k_e and ρ were then obtained from Equations 37 and 1 respectively. The values are given in Table 3.

5. Void

The only factor that changed significantly, besides B_m^2, due to the introduction of a void was assumed to be the thermal utilization factor, f. Hence the condition is similar to that for the addition of a poison. The reactivity was calculated using the same procedure outlined for a poison (cf. VI.D.3). The value of B_m^2 used is given in Table 3 and the values of k_e and ρ are given in Table 3 for configuration 5.

VII. RESULTS AND DISCUSSION

A summary of the experimental and theoretical results are recorded in Table 3. The values of quantities used in the calculations and their sources are listed in Table 4. The measured counting rates for given positions for the reference configuration are tabulated in Table 6 in Appendix B. The horizontal distribution of the neutron flux (proportional to the counting rate) in the x direction of the subcritical assembly for the configurations investigated are shown in Figures 5 and 6 and Figures 9 through 16. The flux distributions are shown for y = 0, y = ± 12 in. and ± 18 in. The flux distribution for these values of y represents an average of the flux measurements for the given y positions. The distribution of neutron flux for the reference configuration is shown for comparison in each figure.

The distribution of the neutron flux in the y direction for configuration 1 is shown in Figures 7 and 8. These figures were plotted to obtain the dimension b, which includes the extrapolated distances, in the y direction and to show that the flux variation in the y direction was symmetrical about the origin. The flux distributions are shown for x = 0, x = ± 12 in. and ± 24 in. and are the average of the flux for the positive and negative positions.

The neutron flux distribution for the 24 in. and 48 in. levels are plotted separately for each configuration to show

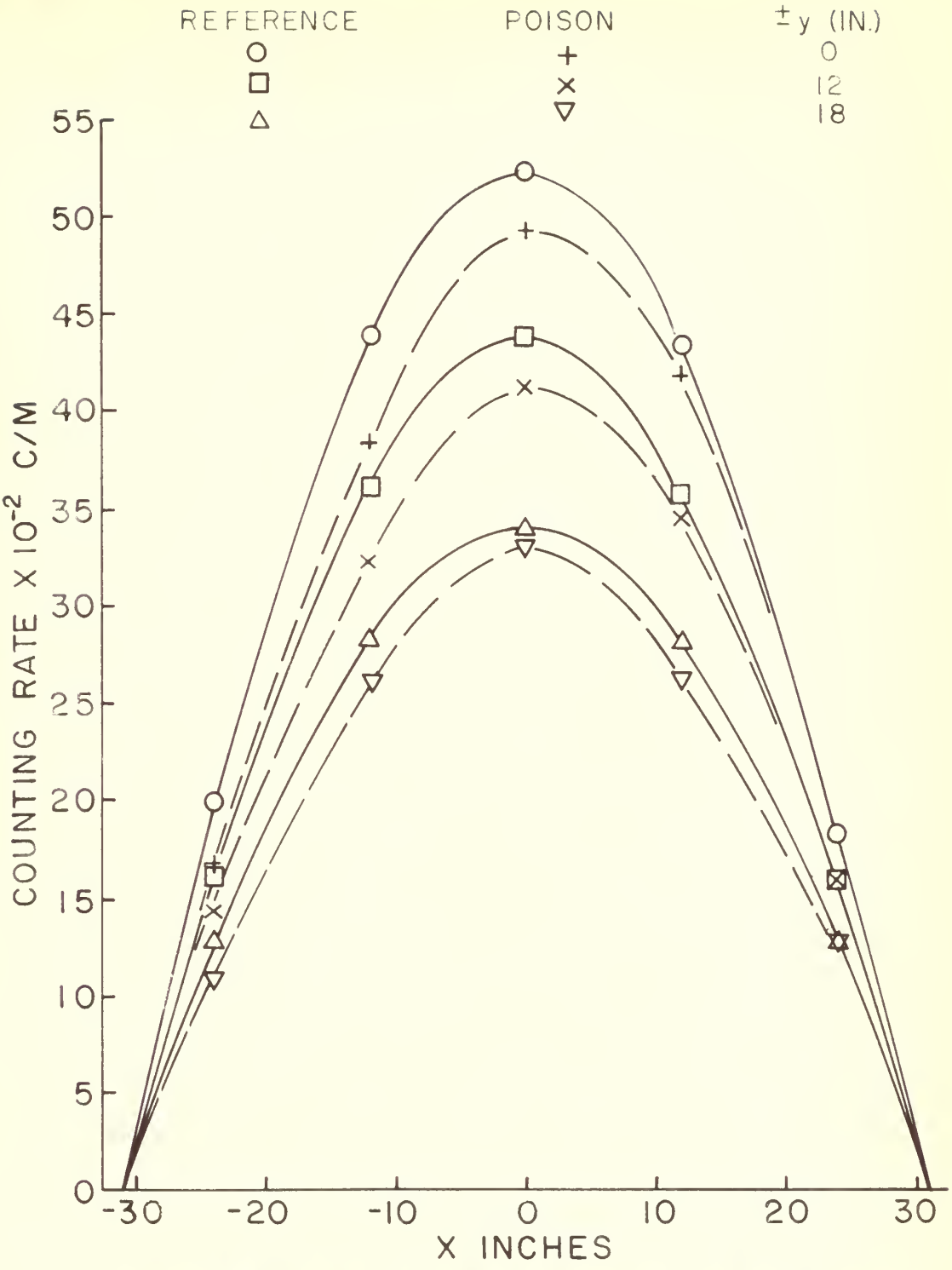

Figure 9. Horizontal flux survey, 48 in. level, configuration 2

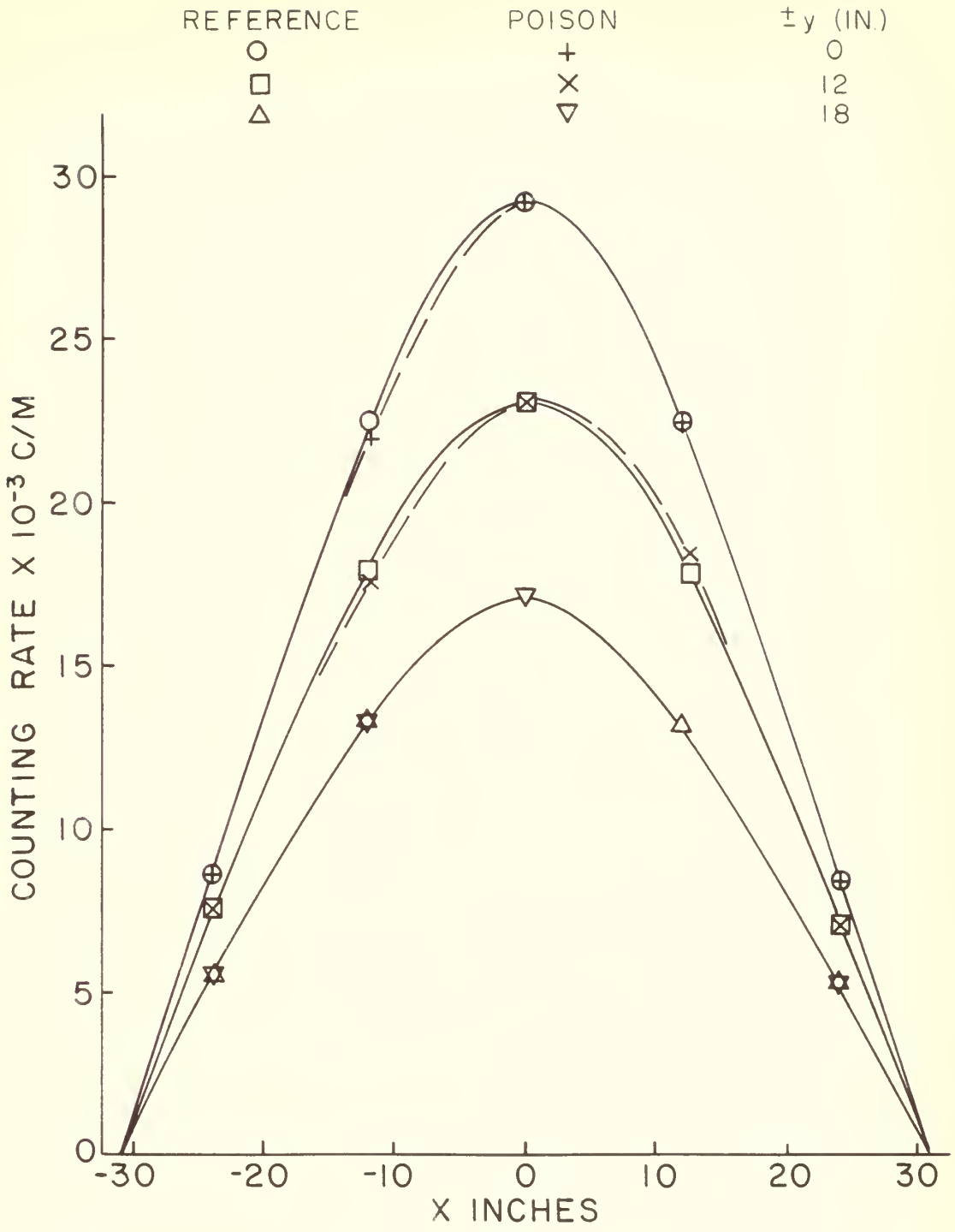

Figure 10. Horizontal flux survey, 24 in. level, configuration 2

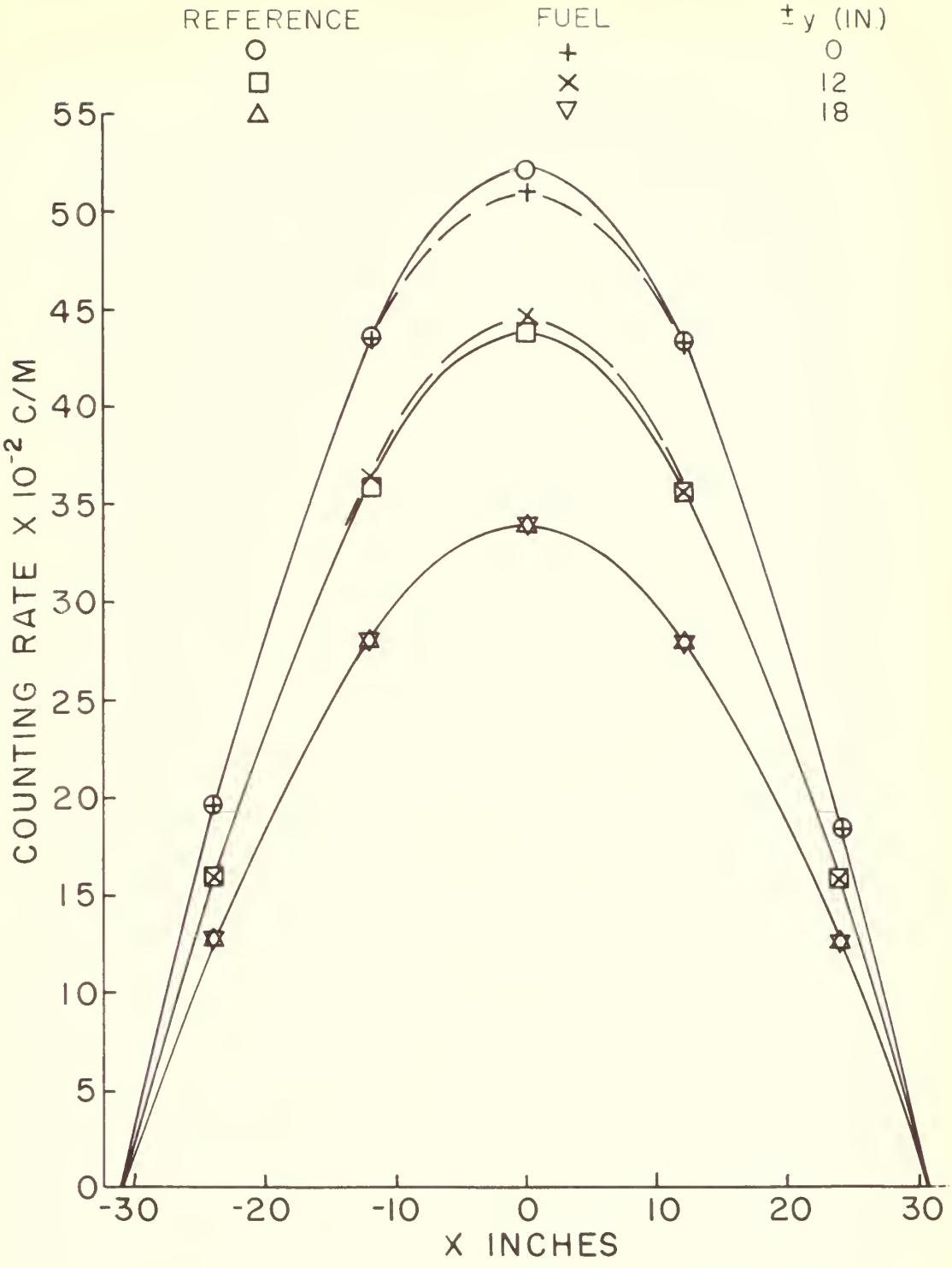

Figure 11. Horizontal flux survey, 48 in. level configuration 3

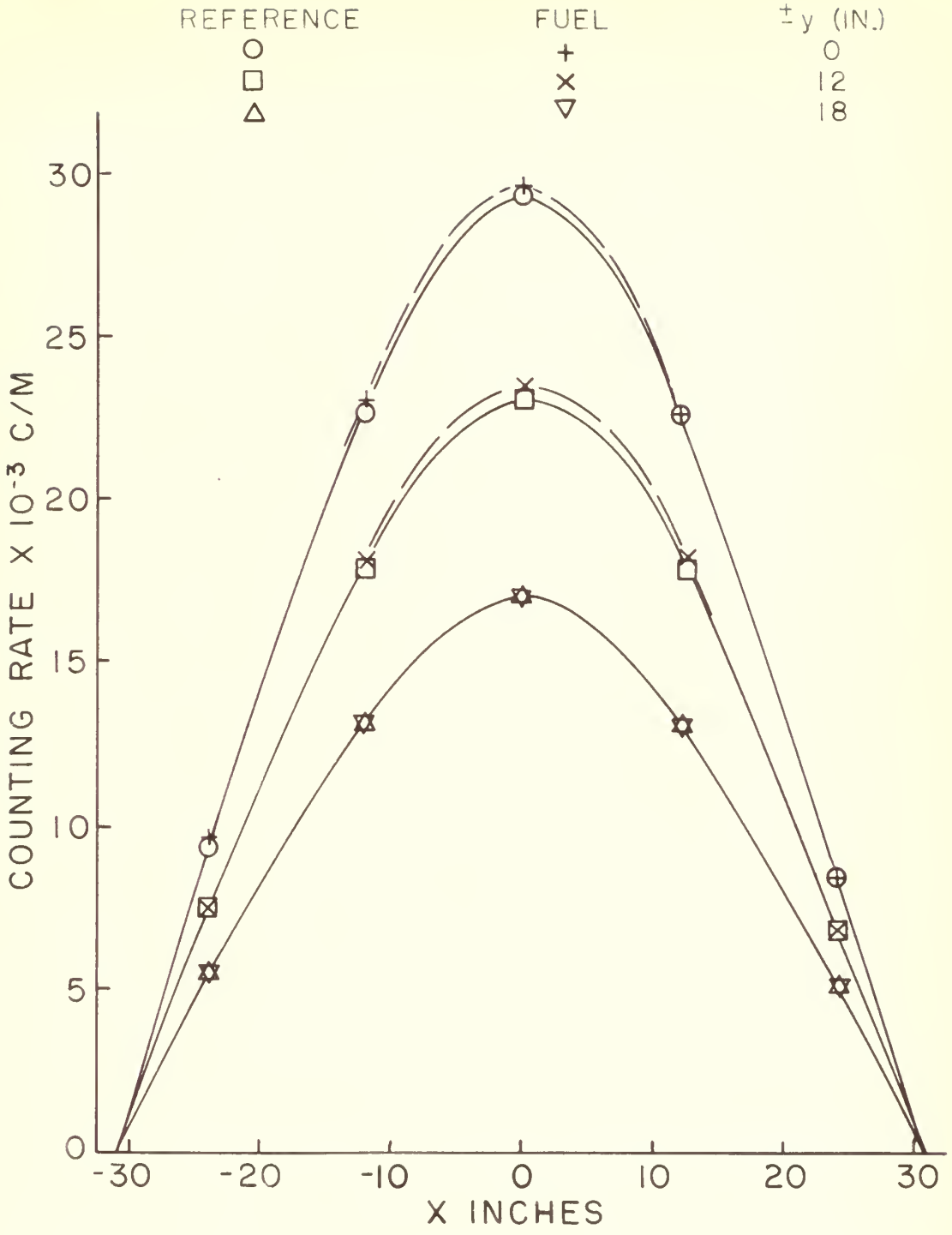

Figure 12. Horizontal flux survey, 24 in. level, configuration 3

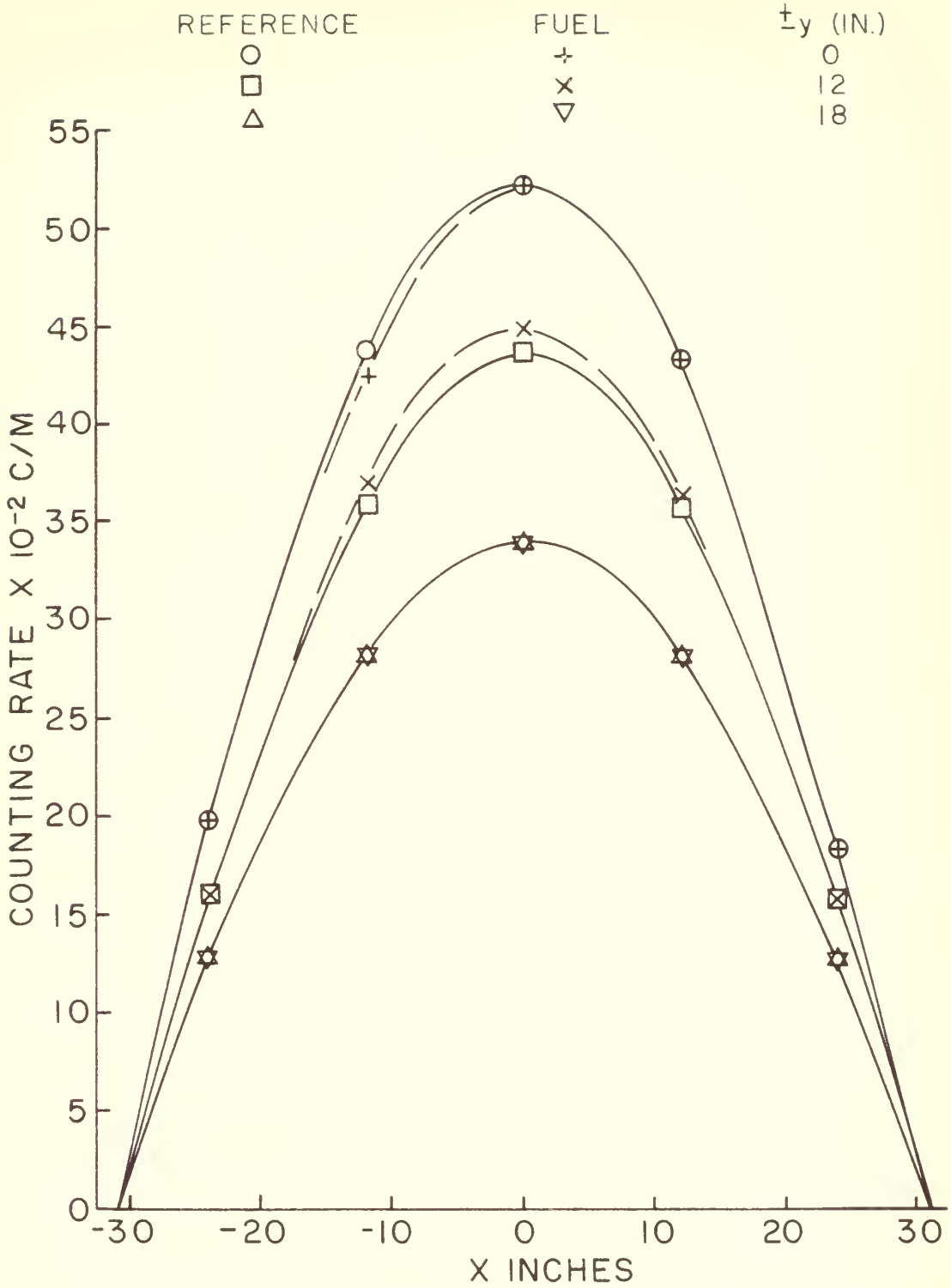

Figure 13. Horizontal flux distribution, 48 in. level, configuration 4

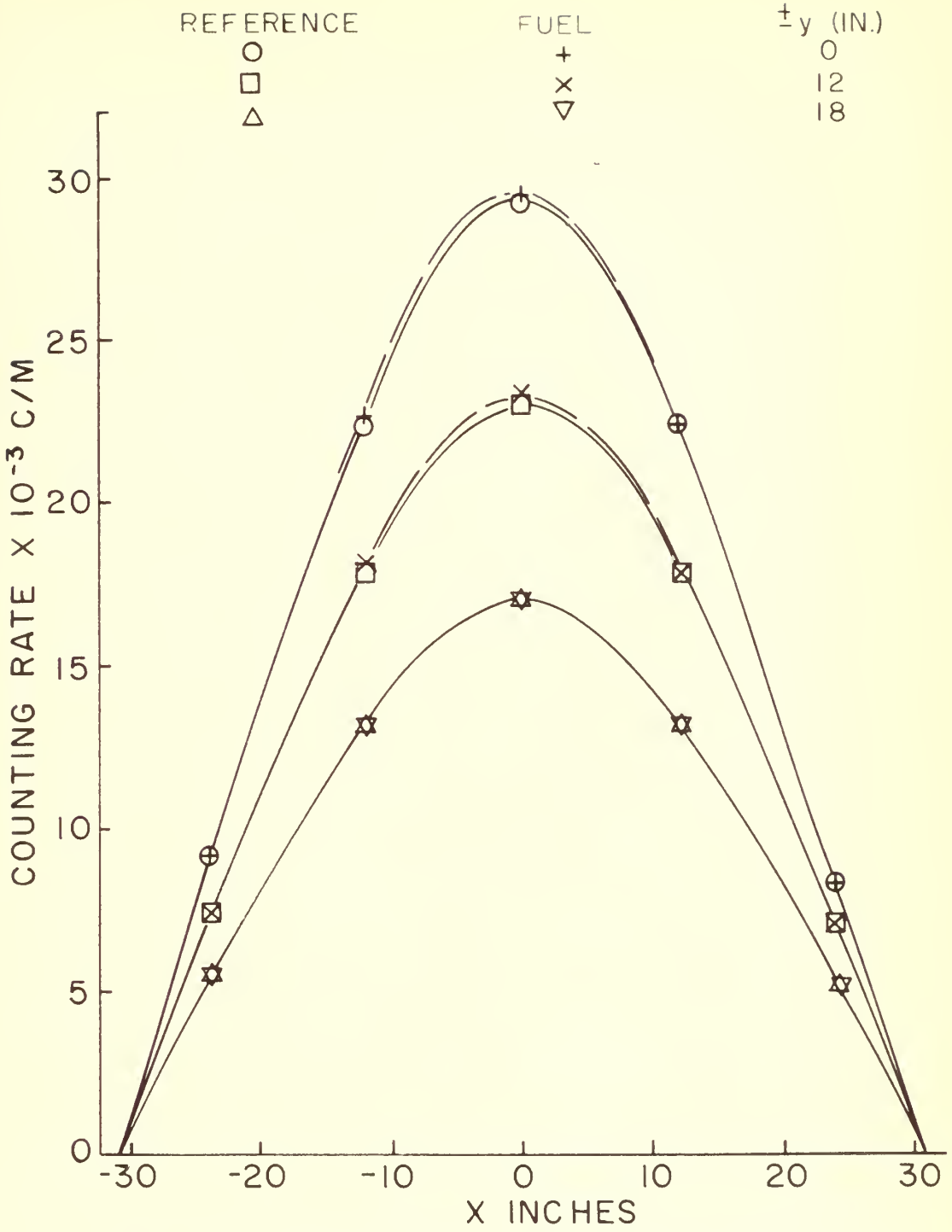

Figure 14. Horizontal flux survey, 24 in. level, configuration 4

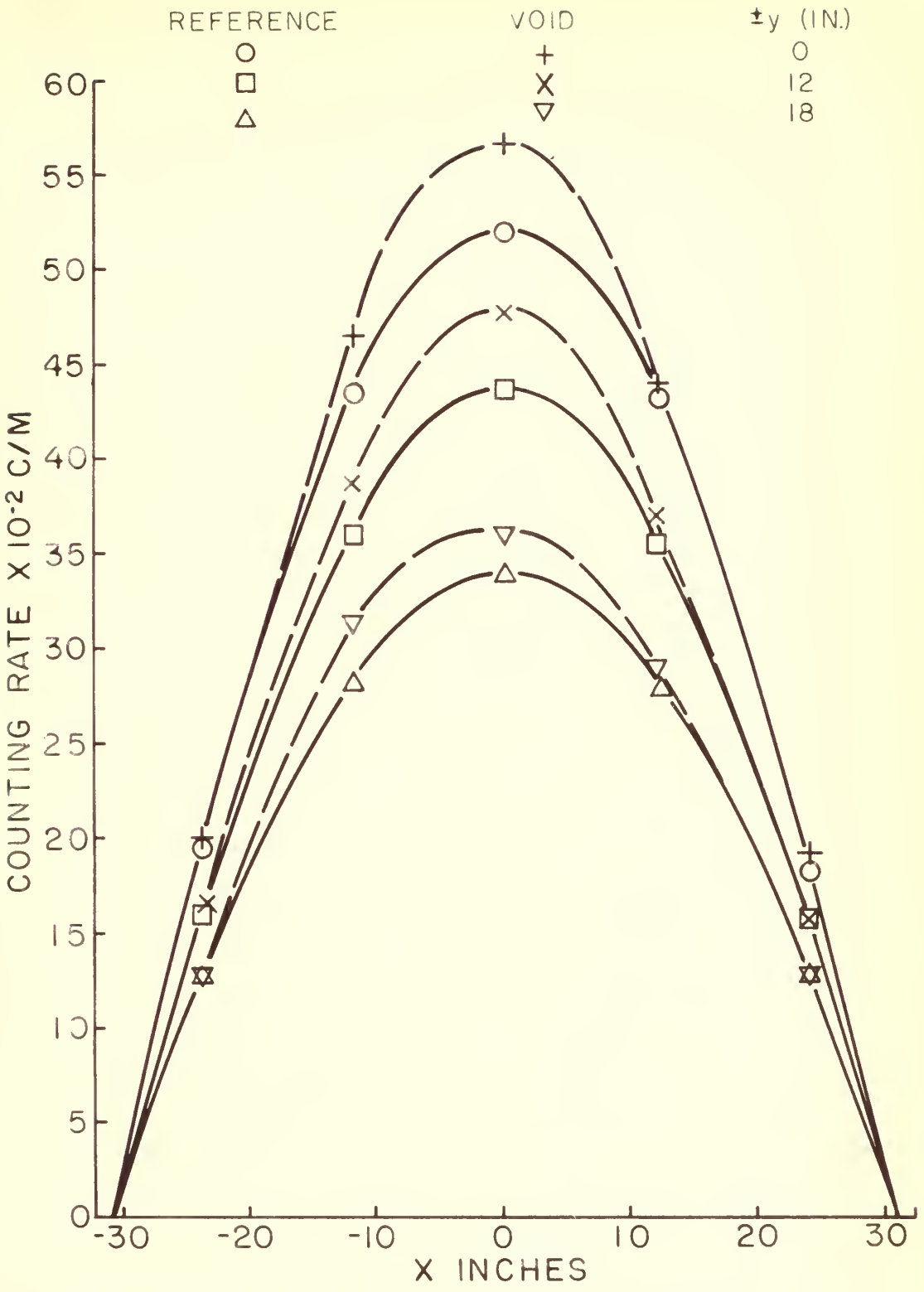

Figure 15. Horizontal flux survey, 48 in. level, configuration 5

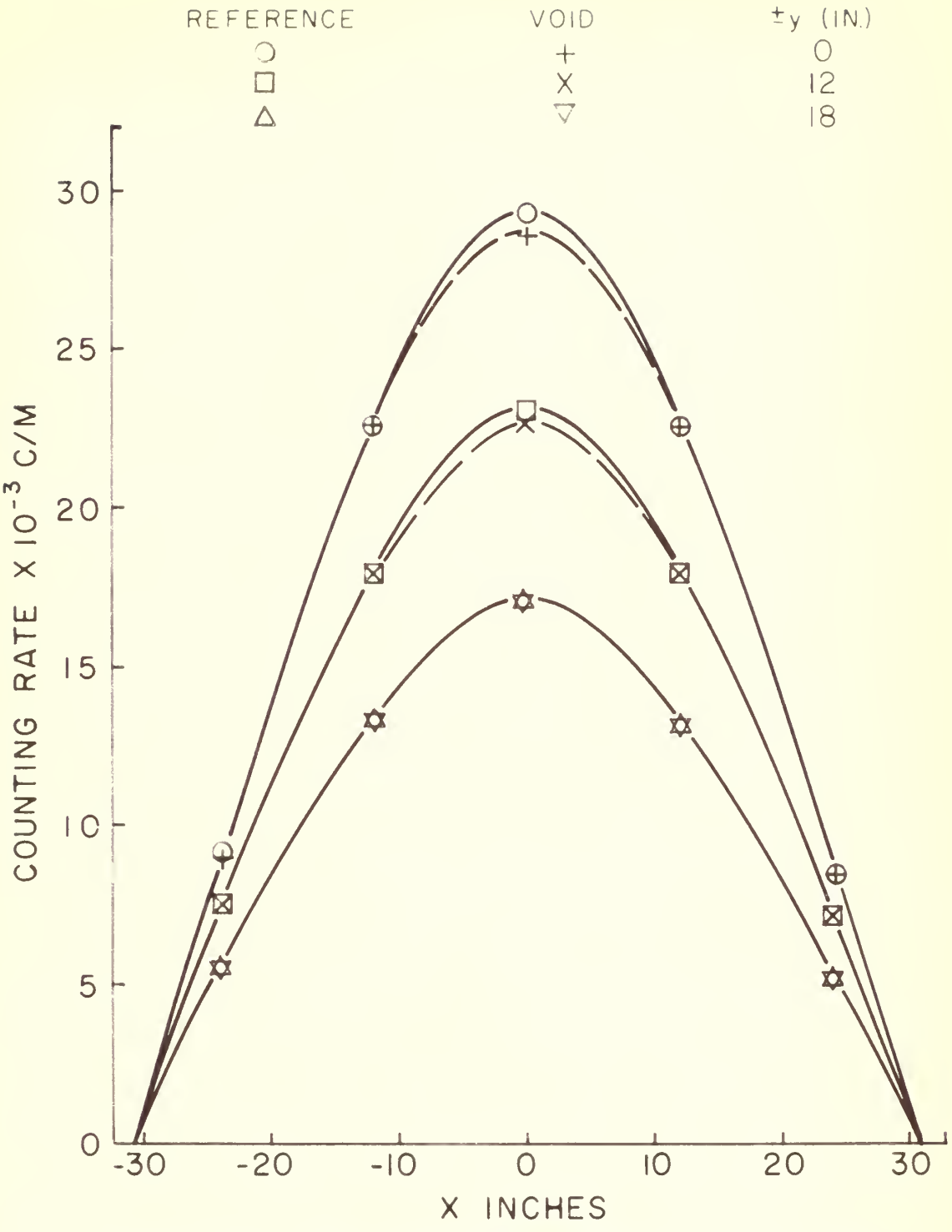

Figure 16. Horizontal flux survey, 24 in. level, configuration 5

Table 3. Summary of results

Ratio of reactivities	Poison: Experimental	Theoretical: Weighting factor ϕ^2	Theoretical: Weighting factor ϕ
$\frac{\rho(\text{configuration 1})}{\rho(\text{configuration 2})}$	1.75	1.48	1.22
$\frac{\rho(\text{configuration 1})}{\rho(\text{distributed})}$	1.49 [a]	0.340	1.19
$\frac{\rho(\text{configuration 2})}{\rho(\text{distributed})}$	0.850 [a]	0.230	0.975

Configuration	Fuel - Theoretical: $B_n^2 \times 10^6$ (cm^{-2})	Weighting factor
3	71.61	ϕ
3	71.96	ϕ^2
4	71.91	ϕ
4	71.99	ϕ^2

Configuration	Experimental: γ ($in.^{-1}$)	Experimental: $B_m^2 \times 10^6$ (cm^{-2})	k	k_e	ρ
reference	0.0671	72	1.051	0.538	-0.860
1	0.0718	-23	0.855	0.334	-1.99
2	0.0708	2	0.986	0.468	-1.14
3	0.0680	56	1.038	0.530	-0.887
4	0.0675	67	1.049	0.535	-0.870
5	0.0644	128	1.090	0.732	-0.366
distributed [a]	-	-	0.954	0.426	-1.34

[a]Values for the distributed poison were calculated using the procedure given in Section VI.D.3.

Table 4. Quantities used in calculations

Symbol	Value	Source
a	62 in.	Measured (cf. Section V.I.C)
b	64 in.	Measured (cf. Section V.I.C)
B_p^2	$41 \times 10^{-6} cm^{-2}$	(9) for 6.00 in. lattice
c	79.75 in.	Measured (cf. Section (VI.D.1)
f	0.863	(9) for 8.48 in. lattice and Equations 34 through 36
L^2	$345\ cm^2$	(9) for 8.48 in. lattice and Equation 36
L_g^2	$2520\ cm^2$	(7)
N_p	4.64×10^{22} nuclei/cm^3	(10)
N_u	4.78×10^{22} nuclei/cm^3	(10)
λ_t	2.7 cm	(7)
σ_a^p	154 barns	(10)
σ_a^u	0.364 barns	(10)
τ	$364\ cm^2$	(7)

more clearly the perturbed neutron flux with respect to the unperturbed flux (reference configuration) for the 24 in. level.

In discussing the results, the perturbed flux distribution due to the addition of the poison, fuel and introduction of the void are compared with the unperturbed, or reference, flux distribution. The theoretical and experimental values

of reactivity and buckling are then compared.

Due to the addition of the poison (configuration 1 and 2) the neutron flux was depressed considerably at the 48 in. level, as shown in Figures 5 and 9 but was depressed only slightly at the center of the 24 in. level (Figures 6 and 10). The flux depression for both levels was due to the presence of the cadmium, which has a high capture cross section for thermal neutrons. The large flux depression in the 48 in. level may be attributed to the large percentage of source neutrons that are absorbed in the poison before arriving at the upper level.

The 24 in. level is below the poison and, therefore, the poison has a negligible effect on the number of source neutrons at the lower level. The slight flux depression in the lower level is attributed to the absorption by the poison of the neutrons produced in the fuel elements of the assembly.

Due to the addition of fuel, configurations 3 and 4, the neutron flux was depressed slightly near the center and was increased slightly at $y = \pm 12$ in. at the 48 in. level, as shown in Figures 11 and 13. The flux was unaltered at distances beyond $y = \pm 18$ in. and $x = \pm 12$ in. The flux distribution with the fuel located at $x = -12$ in., configuration 4, was not symmetrical, but the peak was shifted toward the slugs.

The perturbed flux distribution at the 48 in. level may be explained as follows. In the fuel slugs, non-fission capture occurs in the aluminum casing for thermal neutrons and in the U^{238} for thermal and resonance neutrons. The U^{235} in the added fuel slugs produces fast fission neutrons due to the absorption of thermal neutrons. The number of fast fission neutrons thermalized is a function of distance for a given moderator. If τ is taken equal to 364 cm^{-2} for graphite, the minimum distance for virtually complete thermalization is about 50 cm or 20 in. (1, p. 284). The 48 in. level was 12 in. from the added fuel. A considerable number of the fast fission neutrons produced by the added fuel will be thermalized at the 48 in. level. It is concluded that at the center of the 48 in. level the neutron absorption of the added fuel slugs has a greater effect than the neutron production of the added fuel slugs. In contrast, at y = $\pm$ 12 in. the increase in neutron flux may be attributed to the production of neutrons by the added fuel slugs outweighing their absorption effect.

At the 24 in. level the addition of fuel resulted in an increase in the neutron flux from the center to y = $\pm$ 18 in. and x = $\pm$ 12 in., as shown in Figures 12 and 14. This is in agreement with the previous discussion since the fuel was above the 24 in. level, and thus the absorption of the fuel had very little effect on the flux. Therefore, the produc-

tion of neutrons by the fuel is the more important factor, resulting in an increase in the thermal neutron flux at the lower level.

The unsymmetrical distribution of the neutron flux for configuration 4 (Figures 13 and 14) is due to the off-center position of the fuel at x = - 12 in.

The introduction of a void, configuration 5, resulted in a large increase in the thermal neutron flux throughout the center area of the 48 in. level (Figure 15). The increased flux is due to the decreased neutron absorption in air compared to graphite. The macroscopic absorption cross section of air was calculated to be about 1/10 the macroscopic absorption cross section of graphite.

The neutron flux in the center of the 24 in. level was slightly depressed due to the introduction of the void (Figure 16). The decreased flux is attributed to the decrease in the number of neutrons reflected back to the lower level.

The effect of placing a poison, or absorber, in the assembly was determined theoretically by computing the ratio of reactivities for the same poison placed in two locations and by computing the ratio of reactivities of localized to uniformly distributed poisons. The ratio of the reactivities for configuration 1 to configuration 2 was computed using Equation 18 with a value of γ for the reference configuration (Table 3) and values of a, b and c listed in Table 4.

The ratio was found to be 1.48, which is about 16 percent lower than the experimentally determined value of 1.75 for the same ratio. The ratio of reactivities for a localized to a uniformly distributed poison was determined theoretically for configurations 1 and 2 using Equation 20. The computed ratios are recorded in Table 3 under the weighting factor of ϕ^2. The theoretical values of the ratios are about one-third the experimental values. Since the theoretically determined ratios for a localized to distributed poison using a weighting factor of ϕ^2 did not agree very closely to the experimentally determined ratios, the ratios were computed using a weighting factor of ϕ. The resulting ratios of reactivities for the localized to distributed poison for a weighting factor of ϕ (Table 3) agreed much more closely than the ratios for the weighting factor of ϕ^2. The ratio of reactivities for configuration 1 to configuration 2 was then computed using a weighting factor of ϕ in place of ϕ^2 in Equation 18 and found to be 1.22. It is apparent from a comparison of the values of the various ratios recorded in Table 3 that the weighting factor of ϕ gave theoretical results in closer agreement to the experimental results for the ratios of localized to distributed poisons than did the weighting factor of ϕ^2. However, the agreement between the theoretical and experimental results for these factors were reversed for the ratio of reactivities for configuration 1

to configuration 2.

The following factors could have affected the experimental results. The value of the thermal diffusion length in graphite, L_g^2, and the Fermi age of the thermal neutrons, τ, used in the calculations were obtained from the literature (7). The constant $\eta\varepsilon p$ used in the calculations was based upon the assumption that only f, B_m^2 and L were changed appreciably due to the addition of a poison. The method of experimentally determining γ from the measured neutron flux requires that the flux not be directly affected by the local disturbance. Of the above factors that entered in the experimental determination of reactivity, the one considered most likely to have caused the greatest error is the possibility that the measured neutron flux was directly affected by the absorber. It is difficult to estimate the magnitude of the error introduced by the above factors.

The theoretical method employed had the following probable errors. The perturbed region was assumed small and the values of the original and disturbed neutron flux were assumed to be the same. The weighting factor of ϕ^2 was based upon theory for a critical reactor and only the value of f and B_m^2 were assumed to change due to the addition of the poison.

The effect of adding fuel, configurations 3 and 4, was determined by a comparison of theoretically and experimental-

ly computed values of buckling. The theoretical value of buckling for the added fuel, B_n^2, was calculated using Equation 23 with a value of B^2 for the reference configuration and a value of B_p^2 for a 6.00 in. lattice as given in Table 4. The lattice in the perturbed region was determined to be 6.00 in. from Figure 17. The limits of integration over the volume V_p for configuration 3 were -6 to 6 in. and 30 to 42 in. in the x and z directions respectively, as shown in Figure 17. Since the center of the fuel was placed directly above the origin of coordinates and its length was oriented in the y direction, the limits of integration in the y direction were -12 to 12 in., the length of the added fuel. For configuration 4, the fuel was located horizontally 12 in. in the negative x direction from its location for configuration 3. The limits of integration in the y and z direction were the same as configuration 3 and were from -24 to -12 in. in the x direction.

The theoretical change in buckling determined from Equation 23, with a weighting factor of ϕ^2, was insignificantly small compared to the experimentally determined change in buckling (Table 3). A weighting factor of ϕ was used in place of ϕ^2 in Equation 23 and the change in buckling calculated. This value was about 10 times as great as the value for the change in buckling obtained using a factor of ϕ^2. However, the change in buckling was still very small compared

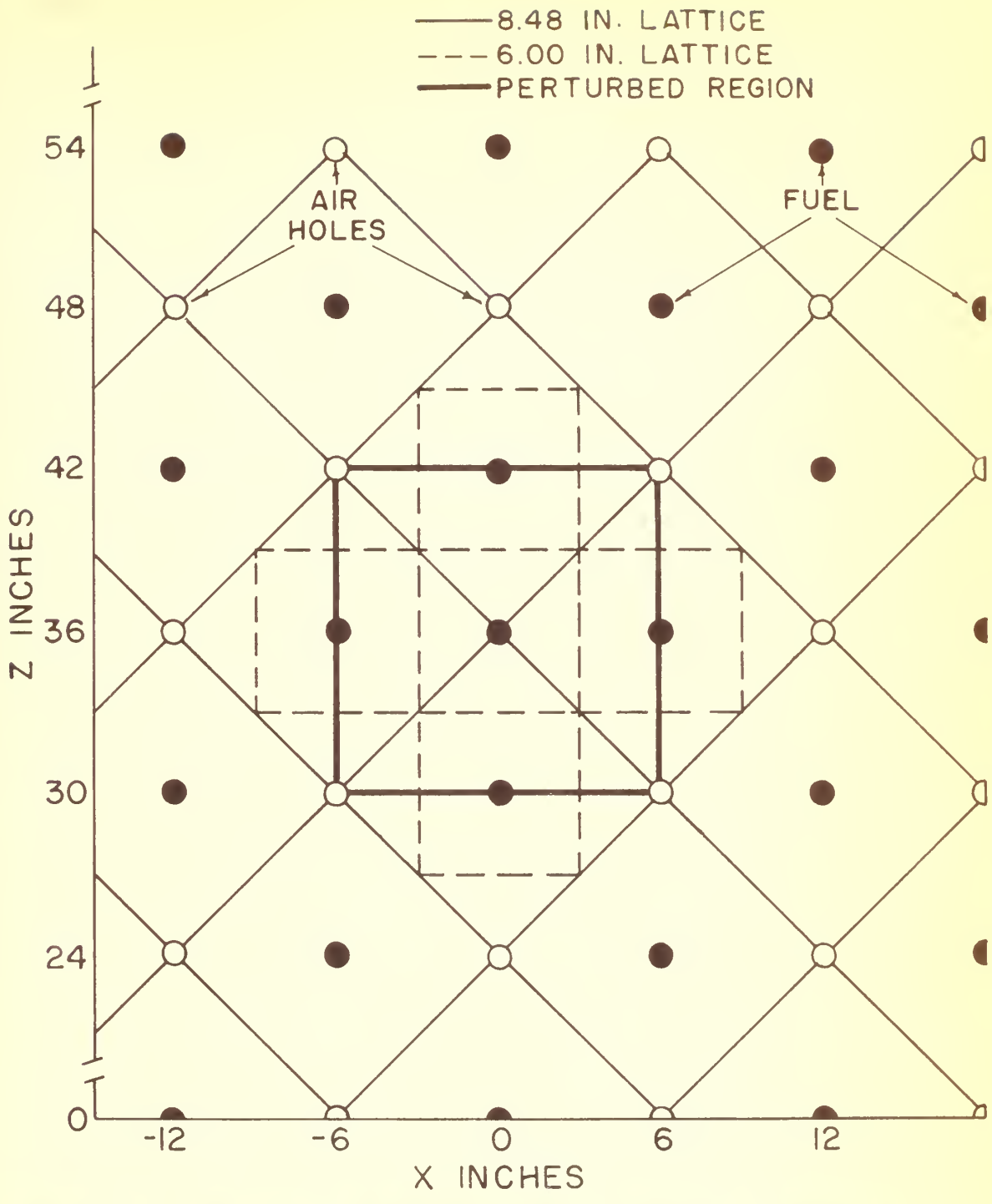

Figure 17. Vertical cross section of center of assembly showing the perturbed region for the addition of fuel

to the experimentally determined change in buckling. It is possible that the experimentally determined value of γ, and thus buckling, could be in error if the measured neutron flux had been directly influenced by the added fuel. This is not considered likely, however, since the flux was not greatly perturbed due to the addition of the fuel. The difference in the values of buckling is attributed to the use of either an improper weighting factor or an incorrect perturbed volume, V_p, in the theoretical calculations.

The reactivity and buckling for the introduction of a void were determined experimentally to be -0.366 and 128 x 10^{-6} cm^{-2} respectively (Table 3). The experimental results were not checked by theory but appear to be in error. The experimental value of buckling for the introduction of the void is considerably greater than the buckling for the unperturbed condition (Table 3). If this were true, a smaller size critical reactor would be possible when a void is introduced. The most probable error in the results is attributed to the direct influence of the void on the neutron flux measurements.

The standard deviation of γ was computed to insure that the change in γ for the different configurations was significant. The standard deviation of γ was calculated for the reference configuration and configuration 3 by the method shown in Appendix A. It was not determined for the other configurations since the values of $\overline{\sigma_{F_1}}$ and $\overline{\sigma_{F_2}}$ for all the

configurations would be nearly the same and thus σ_γ for all the configurations would be almost identical. The standard deviation in γ was determined to be less than 0.00015 $in.^{-1}$. The smallest difference of γ for any two configurations was about three times as great as σ_γ; therefore, the changes in γ are considered significant.

The standard deviation in the measured counting rates was calculated and determined to be smaller than the vertical dimension of the symbols in Figures 5 through 16.

VIII. CONCLUSIONS

The reactivity changes owing to localized perturbations in a subcritical assembly predicted by perturbation theory based upon a weighting factor of ϕ^2 were in reasonable agreement only for the poison located in two positions. The ratio of reactivities predicted theoretically for the same poison at two locations using a weighting factor of ϕ^2 was about 16 percent lower than the experimentally determined value. The same ratio calculated theoretically using a weighting factor of ϕ was 30 percent lower than the experimentally determined value. However, the results for a localized and uniformly distributed poison based upon a weighting factor of ϕ were in much closer agreement with the experimental results than were the theoretical results based upon a factor of ϕ^2. It appears that for the addition of a poison perturbation theory based upon a weighting factor of ϕ gives results in closer agreement with experimental results than does a weighting factor of ϕ^2.

Theoretically predicting the effect of additional fuel using a weighting factor of ϕ or ϕ^2 is considered to give results which are much too low.

The experimental results indicate an increase in buckling due to introducing a void. The result is considered to be erroneous and the error is attributed to the measured neutron flux having been directly affected by the void.

Since it is not known if the experimental measurements of the neutron flux were directly influenced by the local disturbance, it is difficult to ascertain the validity of perturbation theory applied to a subcritical assembly. The usefulness of the subcritical assembly as a test facility is dependent upon the development of experimental methods of determining buckling for localized disturbances to insure accurate and reliable results.

IX. SUGGESTIONS FOR FURTHER STUDY

Studies of additional localized perturbations of the subcritical assembly are needed to properly evaluate the usefulness of perturbation theory to predict reactivity changes in a subcritical assembly. Investigations should be made for a variety of localized changes and the experimental results correlated with theory.

Perturbation theory based upon a critical reactor which can be found in the literature could be investigated further. Perturbation theory applicable to a subcritical assembly has not been developed to the author's knowledge. However, a possible approach might be similar to that presented by Weinberg and Wigner (2, p. 538) for a "burst of neutrons". Although the development is given for a critical reactor, the variation of neutron flux with time is similar to that in a subcritical assembly. It is significant that the weighting factor for this case is ϕ rather than ϕ^2.

Further study and experimentation must be undertaken to determine the minimum distance from the localized perturbation that horizontal neutron flux measurements can be made without being directly affected by the localized disturbance. This can best be done experimentally by comparing the results of measurements taken at pairs of levels at increased distances from the same disturbance.

X. LITERATURE CITED

1. Glasstone, S., and Edlund, M. C. The elements of nuclear reactor theory. Princeton, N. J. D. Van Nostrand Co., Inc. 1952.

2. Weinberg, A. M. and Wigner, E. P. The physical theory of neutron chain reactors. Chicago, Ill. The University of Chicago Press. 1958.

3. McMurry, H. L. Perturbation theory and applications. U.S. Atomic Energy Commission Report AECD-3656 [Technical Information Service, AEC]. [Office of Technical Services, Washington, D. C.] June 11, 1952.

4. _____. Perturbation theory and applications. I. Theoretical. U.S. Atomic Energy Commission Report IDO-16252 [Idaho Operations Office, AEC]. [Office of Technical Services, Washington, D. C.] January 11, 1956.

5. Webster, J. W. An analysis of the accuracy of perturbation theory. U.S. Atomic Energy Commission Report IDO-16173 [Idaho Operations Office, AEC]. [Office of Technical Services, Washington, D. C.] June 17, 1954.

6. _____. Weighting functions for calculating reactivity perturbations in the MTR. U.S. Atomic Energy Commission Report IDO-16095 [Idaho Operations Office, AEC]. [Office of Technical Services, Washington, D. C.] May 14, 1953.

7. Murray, R. L. Nuclear reactor physics. Englewood Cliffs, N. J. Princeton-Hall, Inc. 1957.

8. Galanin, A. D. Teoriya yadernykh reaktorov na teplovykh neitronakh (Theory of thermal-neutron nuclear reactors.) In English translation. New York, N. Y. Consultants Bureau, Inc. c1958.

9. Hoganson, J. H. Operating characteristics of a uranium graphite subcritical assembly with coolant simulation. Unpublished M.S. Thesis. Ames, Iowa. Iowa State College Library. 1957.

10. Davis, M. V. and Hauser, D. T. Thermal-neutron data for the elements. Nucleonics 16, No. 3: 87-89. March 1958.

11. Worthing, A. G. and Geffner, J. Treatment of experimental data. New York, N. Y. John Wiley and Sons, Inc. 1943.

XI. ACKNOWLEDGMENTS

I am deeply indebted to Dr. Robert E. Uhrig for his initial suggestion of this thesis project and for his generous assistance throughout all phases of the work.

I wish to express my sincere thanks to Dr. Glenn Murphy for his guidance and help during my stay at Iowa State College.

My work at Iowa State College was my final year of study in the Aeronautical Engineering Curriculum of the United States Naval Postgraduate School, Monterey, California. I would, therefore, like to express my appreciation to the Navy and in particular to the Naval Postgraduate School for the opportunity of receiving this advanced education.

XII. APPENDIX A: STANDARD DEVIATION OF INVERSE RELAXATION LENGTH

The standard deviation of the inverse relaxation length was determined using the method of propagation of precision indexes as given by Worthing and Geffner (11, p. 208). The standard deviation of γ is

$$\sigma_\gamma = \sqrt{\left(\frac{\partial \gamma}{\partial R}\right)^2 \sigma_R^2} \qquad \text{(A-1)}$$

where R is given by Equation 27. The standard deviation of the ratio R, σ_R, can be obtained from

$$\left(\frac{\sigma_R}{R}\right)^2 = \left(\frac{\sigma_{F_1}}{F_1}\right)^2 + \left(\frac{\sigma_{F_2}}{F_2}\right)^2 \qquad \text{(A-2)}$$

where,

$$\sigma_F^2 = \left(\frac{\partial F}{\partial \phi_1}\right)^2 \sigma_{\phi_1}^2 + \left(\frac{\partial F}{\partial \phi_2}\right)^2 \sigma_{\phi_2}^2 + \ldots . \qquad \text{(A-3)}$$
$$\ldots . + \left(\frac{\partial F}{\partial \phi_i}\right)^2 \sigma_{\phi_i}^2$$

Since

$$F = \sum_{-a/2}^{a/2} \sum_{-b/2}^{b/2} \phi \cos \frac{\pi x}{a} \cos \frac{\pi y}{b} \Delta x \Delta y \qquad \text{(A-4)}$$

and

$$\sigma_\phi = \sqrt{\frac{\phi}{t}} \qquad \text{(A-5)}$$

Equation A-3 becomes

$$\sigma_F^2 = \left(\cos\frac{\pi x_1}{a}\cos\frac{\pi y_1}{b}\,\Delta x\,\Delta y\right)^2 \frac{\phi}{t} + \left(\cos\frac{\pi x_2}{a}\cos\frac{\pi y_2}{b}\,\Delta x\,\Delta y\right)^2 \frac{\phi_2}{t}$$

$$+ \ldots\ldots + \left(\cos\frac{\pi x_i}{a}\cos\frac{\pi y_i}{b}\,\Delta x\,\Delta y\right)^2 \frac{\phi_i}{t} \qquad \text{(A-6)}$$

The squared terms in parentheses in Equation A-6 are the squares of the factors given in Table 1. The standard deviation of the inverse relaxation length for the reference configuration and configuration 3 were calculated using Equations A-1, A-2 and A-6. The values are recorded in Table 5.

Table 5. Standard deviation in

Configuration	$\sigma_{F_1}^2$	$\sigma_{F_1}^2$	σ_R^2	σ_γ
Reference	22,464	4,344	1.01×10^{-4}	0.825×10^{-4}
3	68,159	12,926	3.14×10^{-4}	1.43×10^{-4}

XIII. APPENDIX B: TYPICAL TEST DATA

Table 6. Horizontal flux survey, reference configuration (counting rate C/M)

y (in.)	Row A	Row B	Row C	Row D	Row E
			24 in. level		
21	4,232	10,396	13,239	10,049	3,985
18	5,380	12,350	16,513	12,871	5,125
12	7,235	17,363	22,810	17,472	6,750
6	8,497	21,011	27,279	21,142	7,821
0	9,160	22,675	29,369	22,660	8,411
0	9,175	22,720	29,327	22,547	8,417
-6	8,765	21,596	27,926	21,133	8,069
-12	7,505	18,274	23,331	17,917	7,002
-18	5,735	13,792	17,569	13,223	5,166
-21	4,426	10,813	13,784	10,719	4,313
			48 in. level		
21	1,007	2,173	2,815	2,313	1,002
18	1,236	2,793	3,385	2,709	1,200
12	1,591	3,551	4,381	3,521	1,603
6	1,841	4,100	5,092	4,112	1,819
0	1,996	4,333	5,195	4,333	1,834
0	1,961	4,350	5,258	4,316	1,837
-6	1,857	4,240	5,033	4,066	1,805
-12	1,658	3,597	4,388	3,604	1,548
-18	1,286	2,813	3,367	2,861	1,262
-21	1,058	2,362	2,826	2,361	979